MATHEMATICAL MODELLING OF THE REMOVAL OF ORGANIC MICROPOLLUTANTS IN THE ACTIVATED SLUDGE PROCESS: A LINEAR BIODEGRADATION MODEL

MARK I. NELSON[✉1], RUBAYYI T. ALQAHTANI[2] and FAISAL I. HAI[3]

Abstract

Before wastewaters can be released into the environment, they must be treated to reduce the concentration of organic pollutants in the effluent stream. There is a growing concern as to whether wastewater treatment plants are able to effectively reduce the concentration of micropollutants that are also contained in their influent streams. We investigate the removal of micropollutants in treatment plants by analysing a model that includes biodegradation and sorption as the main mechanisms of micropollutant removal. For the latter a linear adsorption model is used in which adsorption only occurs onto particulates.

The steady-state solutions of the model are found and their stability is determined as a function of the residence time. In the limit of infinite residence time, we show that the removal of biodegradable micropollutants is independent of the processes of adsorption and desorption. The limiting concentration can be decreased by increasing the concentration of growth-related macropollutants. Although, in principle, it is possible that the concentration of micropollutants is minimized at a finite value of the residence time, this was found not to be the case for the particular biodegradable micropollutants considered.

For nonbiodegradable pollutants, we show that their removal is always optimized at a finite value of the residence time. For finite values of the residence time, we obtain a simple condition which identifies whether biodegradation is more or less efficient than adsorption as a removal mechanism. Surprisingly, we find that, for the micropollutants considered, adsorption is always more important than biodegradation, even when the micropollutant is classified as being highly biodegradable with low adsorption.

[1]School of Mathematics and Applied Statistics, University of Wollongong, NSW 2522, Australia; e-mail: mnelson@uow.edu.au.
[2]Department of Mathematics and Statistics, College of Science, Al-Imam University, Riyadh 11566, Saudi Arabia; e-mail: rtaa648@uowmail.edu.au.
[3]Strategic Water Infrastructure Laboratory, School of Civil, Mining and Environmental Engineering, University of Wollongong, NSW 2522, Australia; e-mail: faisal@uow.edu.au.

1. Introduction

Conventional wastewater treatment plants (WWTPs) can effectively remove bulk carbonaceous organic materials as well as nutrients such as nitrogen and phosphorus. However, they were not designed to remove organic pollutants which are detected in trace concentrations, that is, micropollutants [15]. Common micropollutants include chemicals associated with personal care products, such as pharmaceutical compounds and their derivatives, and chemicals associated with domestic use, such as pesticides and surfactants. Other common micropollutants include hormones, metals and polycyclic aromatic hydrocarbons (PAHs). The release of micropollutants into aquatic ecosystems has been shown to have an ecotoxic impact. This has led to European legislation mandating both industry and states to reduce their release [25].

The introduction of relevant legislation has spurred experimental investigations into the removal mechanisms of typical micropollutants. The development of well-analysed mathematical models can provide a tool for decision makers to evaluate the relative importance of the mechanisms which remove micropollutants. These models can also be used to optimize the operation of wastewater treatment plants to significantly reduce the micropollutant concentration downstream of a WWTP. This optimization must be achieved without adversely affecting the removal of "standard" organic pollutants. A literature review outlining current knowledge about the threats posed by micropollutants, detailing current mathematical models, is presented in Section 1.1.

We formulate a mathematical model for the removal of organic micropollutants from municipal wastewaters. The model includes the four main mechanisms leading to micropollutant removal: biodegradation, cometabolism, volatilization and sorption [30]. In this paper, we investigate the special case in which the only removal mechanisms are biodegradation and sorption. Identifying the relative importance of each of these mechanisms is a major challenge for emerging new micropollutants. A surprise from our model is that, for the nine biodegradable micropollutants considered, adsorption is always a more important removal mechanism than biodegradation—even for four micropollutants that have been identified as being "highly biodegradable with low sorption".

1.1. Literature review

Mathematical models for the removal of micropollutants in WWTPs have recently been reviewed by Pomiès et al. [30]. These authors found 18 models published over the period 1989–2010.

There are four main mechanisms by which micropollutants are removed in WWTPs [30]. These are biodegradation, cometabolism, mass transfer into the gas phase and sorption onto particulates. These mechanisms do not necessarily apply to all contaminants. For example, only volatile organic compounds are removed by mass transfer into the gas phase. Additional mechanisms may apply to some contaminants. For example, heavy metals can be removed by precipitation. Identifying the most important removal mechanism for a particular contaminant is one of the applications of mathematical models.

TABLE 1. Micropollutant removal mechanisms included in activated sludge process models. AD: Adsorption. AP: Aqueous biodegradation. BC: Biological conversion. PP: Particulate biodegradation. PPT: Precipitation. DCM: Biodegradation on dissolved and colloidal matter. DES: Desorption. MT: Mass transfer. (S): Removal of the micropollutant is associated with the growth of a specialized biomass, that is, it is considered as a growth substrate for this species. The symbol X indicates that the specified mechanism was included in the model. The superscript (*) indicates that it is assumed that the desorption–sorption process is at equilibrium.

Author	BC			AD	DES	MT	PPT
	AP	PP	DCM				
Abegglen et al. [1]	X	—	—	X	X	—	—
Delgadillo-Mirquez et al. [8]	X	X	X	X	X	X	—
Fernandez-Fontaina et al. [14]	X	—	—	X	X	—	—
Fernandez-Fontaina et al. [12]	X	—	—	X	X	X	—
Jacobsen and Arvin [17]	X	—	—	X	X	—	—
Joss et al. [20]	X	—	—	X	X	—	—
Melcer et al. [26]	X	—	—	X (*)	X(*)	X	—
Parker et al. [29]	—	—	—	X (*)	X(*)	—	X
Siegrist et al. [32]	X (S)	—	—	X	X	—	—
Urase and Kikuta [39]	X	—	—	X	X	—	—

Table 1 summarizes the removal mechanisms that have been included in models. All models, excepting those for heavy metals, include biotransformation and sorption–desorption processes. In Sections 1.1.1–1.1.3, we review the modelling of biodegradation and cometabolism, the processes of adsorption and desorption, and mass transfer, respectively. In Section 1.1.4, we provide a limited review of activated sludge process (ASP) models, restricting our attention to those models that have been used within the context of modelling the removal of micropollutants.

1.1.1 *Modelling the biological removal of micropollutants through biodegradation and cometabolism.* Micropollutants may be removed from WWTPs through the action of biomass. This may be referred to either as the biological conversion of micropollutants or the biotransformation of micropollutants. Two processes by which this transformation can occur are biodegradation and cometabolism. There is no standard definition of what "biodegradation" means in the context of the removal of micropollutants [30]. A common interpretation is that it is the removal of micropollutants in a process which is *not* associated with the growth of the microorganism. Furthermore, it is widely assumed, as shown in Table 1, that biodegradation only happens in the aqueous phase. This assumption has been investigated by Delgadillo-Mirquez et al. [8].

Cometabolism refers to micropollutant degradation in the presence of another easily degradable substrate. In this case the micropollutants do not serve as the source of carbon for microbial growth [7]. Many organic micropollutants present in wastewater treatment plants are biodegraded by a cometabolic mechanism.

The total rate of biological removal (r_{bio} [μg L^{-1} day^{-1}]) is given by the sum of the rate of cometabolism and the rate of biodegradation

$$r_{\text{bio}} = T_C \frac{\mu(S_s)}{Y_H} \cdot \left(\frac{C_s}{K_{SC} + C_s} \right) X + k_c \cdot \left(\frac{C_s}{K_{SC} + C_s} \right) X, \tag{1.1}$$

where the first and last terms on the right-hand side of equation (1.1) are the rate due to cometabolism and the rate due to biodegradation, respectively. In equation (1.1), C_s is the concentration of soluble micropollutants [μg L^{-1}] and X is the concentration of active biomass [g COD L^{-1}]. The specific growth rate, $\mu(S)$ [day^{-1}], of the biomass upon the soluble substrate, S_S [g COD L^{-1}], is given by

$$\mu = \mu_{\text{max}} \cdot \frac{S_s}{K_S + S_s}. \tag{1.2}$$

The remaining constants in equations (1.1) and (1.2) are: K_S [g COD L^{-1}], the Monod half-saturation constant for the growth of heterotrophic biomass; K_{SC}, the half-saturation constant of micropollutants; T_C, the micropollutant transformation capacity, which represents Y_H [(g COD L^{-1})/(g COD L^{-1})], the growth yield; k_c [μg (g COD day)$^{-1}$], the maximum rate of biodegradation of the micropollutant; and μ_{max} [day^{-1}], the maximum growth rate of the biomass.

Equation (1.1) is often simplified by putting the micropollutant transformation capacity equal to zero ($T_C = 0$). This removes the cometabolism term, giving

$$r_{\text{biol}}(T_C = 0) = k_c \cdot \frac{C_s}{K_{SC} + C_s} X. \tag{1.3}$$

This formulation implies that biological conversion of the micropollutant is not associated with growth of the biomass.

The rate functions given in equations (1.1) and (1.3) may be further modified by multiplying them by switching functions which have the effect of turning biodegradation "off" if the concentration of a particular substance is either too "high" (inhibition) or too "low". The use of switching functions to modify growth rates is described in [16].

Micropollutants are generally present at low concentrations in WWTPs. Consequently, the rate of biodegradation may be simplified to

$$r_{\text{biol}}(T_C = 0, C_s \ll K_{SC}) = k_{\text{biol}} C_s X, \tag{1.4}$$

where $k_{\text{biol}} = k_c / K_{SC}$ [L (g COD day)$^{-1}$] is the degradation rate coefficient. (Formally this requires $C_s \ll K_{SC}$.) Under circumstances in which the biomass concentration is constant, equation (1.4) reduces to the first-order rate law

$$r_{\text{biol}}(T_C = 0, C_s \ll K_{SC}, X = \text{constant}) = k'_{\text{biol}} C_s, \tag{1.5}$$

where $k'_{\text{biol}} = k_{\text{biol}} X$ [day^{-1}] is the degradation rate coefficient. This rate expression has been widely used to model the environmental removal of organic pollutants.

TABLE 2. The biotransformation model used to model the biodegradation of a micropollutant.

Author	Cometabolic Monod, equation (1.1)	Monod, equation (1.3)	Second order, equation (1.4)	First order, equation (1.5)
Abegglen et al. [1]	—	—	X	—
Delgadillo-Mirquez et al. [8]	X	X	—	—
Fernandez-Fontaina et al. [14]	—	—	—	X
Fernandez-Fontaina et al. [12]	X	—	—	X
Jacobsen and Arvin [17]	—	X	—	—
Joss et al. [20]	—	—	X	—
Melcer et al. [26]	—	—	X	—
Siegrist et al. [32]	—	X	—	—
Urase and Kikuta [39]	—	—	—	X

Regardless of the model used, it is widely assumed that the micropollutant does not provide a food source for active biomass. This assumption is justified as the micropollutant is only present in trace levels, typically μg L^{-1}, or, to be more precise, when the concentration of the micropollutants is much smaller than the concentration of the soluble substrate.

The use of the rate expressions (1.1) and (1.3)–(1.5) in dynamic models for the biodegradation of micropollutants is summarized in Table 2.

1.1.2 *Modelling adsorption–desorption.* We now turn our attention to the modelling of adsorption–desorption processes. Despite the possible nonlinear behaviour of adsorption, a linear adsorption model is always chosen due to the assumed low concentration of micropollutants. The standard assumption is that adsorption only occurs onto particulates, that is, onto a solid phase. However, based upon experimental evidence, Delgadillo-Mirquez et al. [8] developed a model in which adsorption can also occur onto dissolved and colloidal matter, that is, in the aqueous phase.

1.1.3 *Mass transfer.* Melcer et al. [26] modelled volatilization as being due to two processes: surface volatilization, which is important for transfer from open tanks such as clarifiers, and air stripping, which occurs in aerated turbulent process vessels. Both processes are modelled by terms of the form

$$V\frac{dC_s}{dt} = -VK_{La}(C_s - C_g),$$

where V is a suitable volume [L], t is time [day], K_{La} is a mass transfer coefficient [day^{-1}] and C_g is the gaseous concentration of the micropollutant [μ g COD L^{-1}]. The differences between the two processes is in how the mass transfer coefficient is calculated. If it can be assumed that air movement above the clarifier/vessel is sufficient to carry away volatilized compounds, then the equilibrium water phase concentration of the volatilized compound is negligible, that is, $C_g \approx 0$.

Delgadillo-Mirquez et al. [8] modelled volatilization as an equilibrium process between soluble and gaseous micropollutants with

$$V\frac{dC_s}{dt} = -VK_{La}(HC_s - C_g),$$

where H is Henry's constant [–], which describes the equilibrium between gas phase and the soluble concentration of micropollutant.

Fernandez-Fontaina et al. [12] modelled volatilization by the term

$$V\frac{dC_s}{dt} = -H \cdot Q_{air} \cdot C_s,$$

where Q_{air} is the aeration flow rate [L_{air} day^{-1}]. This formulation assumes that air movement above the aerated vessel ensures that the equilibrium gas-phase concentration of the micropollutant is negligible. This is the approach used in this paper.

1.1.4 *Dynamic models.* In a dynamic model a system of differential equations is written down for the removal of the micropollutant. The alternative is a static model, in which steady-state expressions for the state variables are developed without starting from a system of differential equations. Such models may assume that adsorption–desorption processes reach an equilibrium on a faster time scale than that of other processes.

Static models include those of Byrns [4], Cowan et al. [6], Fernandez-Fontaina et al. [13], Struijs et al. [33], Suarez et al. [34] and Wang et al. [40].

Dynamic models involve state variables associated with the operation of the ASP. Which variables are involved depends upon what assumptions are made but they commonly include soluble substrate, total suspended solids and biomass concentration. A key question is therefore how to model the removal of macropollutants in the ASP.

The simplest approach is not to model the ASP, but to measure the values of the state variables required for the micropollutant submodel. The second approach is to use a simplified model for the ASP consisting of a limited number, typically one or two, biochemical processes. The third approach uses a detailed model for the ASP, such as the activated sludge model no. 1 (ASM1) [16], which has been developed to simulate the removal of nutrients and organic matter in WWTPs. A final approach is to use a "black box" model to simulate the ASP.

In Sections 1.1.4.1–1.1.4.4, we overview how the ASP has been modelled within the context of models for the removal of micropollutants. This is *not* a literature review of ASP models.

1.1.4.1 *No ASP model (experimental measurements).* Micropollutant removal from a batch reactor has been modelled by Abegglen et al. [1], Fernandez-Fontaina et al. [14] and Urase and Kikuta [39]. (Fernandez-Fontaina et al. [14] also investigated removal in a membrane bioreactor.) In [1, 39], the required inputs were the mixed liquor suspended solids concentration and the total suspended solids, respectively. In [14], the required inputs were the biomass concentration and the total solids concentration.

Fernandez-Fontaina et al. [12] developed a model for micropollutant removal based upon cometabolic kinetics by nitrifying biomass. The first-order kinetic model (1.5) was used. The required experimental inputs are the concentrations of biomass, growth substrate and total suspended solids. These models were used to analyse the removal of 12 micropollutants associated with pharmaceutical use. Four of these compounds were found not to be biodegradable. The biotransformation of four of the compounds was found to be more accurately predicted by cometabolic Monod-type kinetics.

1.1.4.2 *Simplified model for the ASP.* The ASP model used by Joss et al. [20] contains a single-step biochemical model. This step is the growth of active biomass by consumption of soluble substrate. Their model was used to investigate the impact of the reactor configuration upon the removal of the micropollutant. It was found that the use of a reactor cascade appreciably improved the removal of nonsorbing and biodegradable micropollutants compared to a single reactor.

The ASP model used by Jacobsen and Arvin [17] and Delgadillo-Mirquez et al. [8] contains a two-step biochemical model. The first step is the hydrolysis of slowly biodegradable particulate substrate to produce soluble substrate. The second step is biodegradation of the soluble substrate through biomass growth. A third process is biomass decay. The model of Jacobsen and Arvin [17] can be viewed as a simplification of the ASM1 [16]. This is not the case for the model of Delgadillo-Mirquez et al. [8]. For example, the models differ in how hydrolysis is modelled. The former models hydrolysis using Contois kinetics whereas in the latter it is described as a first-order process (with respect to the particulate concentration).

A nonstandard assumption made by Jacobsen and Arvin [17] is that the micropollutant is biodegraded not by the "regular" biomass but by a specialized microbial species. The micropollutant subsystem consists of five processes: growth of the specialized biomass by consumption of soluble substrate, biodegradation of the micropollutant by the specialist biomass, decay of the specialized biomass and adsorption and desorption processes associated with the micropollutant. It is assumed that growth of the specialized biomass upon the micropollutant is negligible.

The incorporation of a specialist biomass represents the addition of a specific microbial culture to the ASP with the hope that it will better remove the micropollutant than the "standard" WWTP biomass. This strategy is known as biosupplementation or bioaugmentation.

Delgadillo-Mirquez et al. [8] developed a micropollutant submodel in which the micropollutant can adsorb onto a solid phase, that is, onto particulates, and into

the liquid phase, that is, onto dissolved and colloidal matter (DCM). In addition to biodegradation of the soluble micropollutant, the adsorbed micropollutant, both that adsorbed onto DCM and that adsorbed onto the particulates, may be biodegraded. As the rate of biodegradation in the DCM component is different from that for the soluble micropollutant, indeed it may be zero, the existence of this component can influence the distribution and bioavailability of the micropollutant.

The model was used to investigate two hypotheses. The first compared the use of a cometabolic model for biodegradation against the use of a pure Monod model; the former provided a better fit to experimental data. The second hypothesis tested which compartment is available for biodegradation. The best fit to experimental data was obtained when it was assumed that only soluble micropollutant is available for biodegradation.

1.1.4.3 *A detailed model for the ASP.* Siegrist et al. [32] modelled the ASP using the ASM1 model. A nonstandard assumption is made that the micropollutant (nitrilotriacetate, NTA) is biodegraded not by the "regular" biomass but by a specialized microbial species. Unlike the model developed by Delgadillo-Mirquez et al. [8], discussed in Section 1.1.4.2, which made the same nonstandard assumption, the specialized biomass grows through consumption of both soluble substrate and the micropollutant. Thus, the micropollutant acts as a growth substrate and its removal is associated with the growth of the microorganism, that is, it is not "biodegraded" in the same sense as in the other models discussed in this review.

The micropollutant submodel contains five processes. There are two processes describing the growth of the specialized biomass, the decay of the specialized biomass and the reversible adsorption of the micropollutant onto suspended solids. Associated with these additional processes are three additional state variables: soluble NTA (S_{NTA}), the biomass of NTA degraders ($X_{\mathrm{B,NTA}}$) and adsorbed NTA (X_{NTA}).

The five-process model was too complex to be fitted against experimental data. A simplified scheme, in which two processes were removed, could be fitted against the available data. The removed processes were the growth of NTA degraders upon soluble substrate and decay of the NTA degraders.

1.1.4.4 *A "black box" approach to modelling the ASP.* Melcer et al. [26] and Parker et al. [29] developed models to simulates the operation of activated sludge systems using the TOXCHEM computer package. TOXCHEM describes contaminant removal in the grit chamber, the primary clarifier, the aeration basin and the secondary clarifier.

Melcer et al. [26] developed a model that applies to WWTPs using either diffused or surface aeration. An interesting feature of this model is that mass transfer into the gas phase is modelled through two mechanisms: surface volatilization and air stripping. It is assumed that sorption and desorption are at equilibrium.

The model developed by Parker et al. [29] simulates the removal of metals. Consequently, biodegradation and mass transfer mechanisms are eliminated. Metals are removed by sorption onto biological solids and by precipitation.

2. Biochemical processes

In this section, we describe the biochemical processes and reactions that are included in the model. There are three biochemical reactions. Two of these, equations (2.1) and (2.2), are associated with the activated sludge process. The third reaction, equation (2.3), is the degradation of the micropollutants by the biomass.

The model includes two physical processes. These are sorption of the micropollutants onto the suspended solids to form particulate micropollutants, equation (2.4), and desorption of the particulates, equation (2.5).

Soluble substrate (S_s) is consumed by the biomass ($X_{B,H}$) to produce new biomass

$$S_s \xrightarrow[X_{B,H}]{\mu(S_s)} Y_H X_{B,H}. \tag{2.1}$$

In this equation, the parameter Y_H [(g COD L^{-1})/(g COD L^{-1})] is the heterotrophic yield coefficient.

Death of particulate biomass

$$X_{B,H} \xrightarrow{b_H} \text{decay products}, \tag{2.2}$$

where b_H [day^{-1}] is the heterotrophic decay coefficient. The decay products formed by the decay of particulate matter are not considered in the model.

Biological removal of micropollutants

$$C_s \xrightarrow[X_{B,H}]{k_{\text{biol}}} \text{products}. \tag{2.3}$$

The products formed during the biological removal of micropollutants are not considered in the model.

Sorption

$$C_s + \text{TSS} \xrightarrow{k_{\text{sor}}} C_p. \tag{2.4}$$

In this equation, TSS [g SS L^{-1}] represents the total suspended solids whilst k_{sor} [L (g SS day)$^{-1}$] is the kinetic constant for adsorption.

Desorption

$$C_p \xrightarrow{k_{\text{des}}} C_s + \text{TSS}. \tag{2.5}$$

In this equation, k_{des} [day^{-1}] is the kinetic constant for desorption. The parameter K_d [L (g SS)$^{-1}$] is the equilibrium constant for the sorption–desorption process. By definition,

$$K_d = \frac{k_{\text{sor}}}{k_{\text{des}}}.$$

3. Equations

In line with practical operation, we formulate the model assuming that aeration is tightly controlled so that dissolved oxygen does not limit the growth of biomass; consequently, it is not needed as a state variable.

3.1. The dimensional model The model contains two differential equations for the activated sludge process, equations (3.1) and (3.2), and two equations for the dynamics of the micropollutants, equations (3.3) and (3.4). The rate of change of soluble substrate

$$V\frac{dS_s}{dt} = F(S_{s,\text{in}} - S_s) - \frac{\mu_{\max}}{Y_H} \cdot M_2(S_s) \cdot X_{B,H} \cdot V, \tag{3.1}$$

where the parameters V, F, $S_{s,\text{in}}$ and M_2 are the volume of the bioreactor [L], the flow rate through the bioreactor [L day^{-1}], the substrate concentration in the feed [g COD L^{-1}] and Monod kinetics for readily biodegradable substrate, respectively.

The rate of change of particulate biomass (heterotrophs)

$$V\frac{dX_{B,H}}{dt} = F(X_{B,H,\text{in}} - X_{B,H}) + RF(C - 1)X_{B,H} + \mu_{\max} \cdot M_2(S_s) \cdot X_{B,H} \cdot V - b_H X_{B,H} V, \tag{3.2}$$

where the parameters $X_{B,H,\text{in}}$, C and R are the concentration of particulate biomass in the feed [g COD L^{-1}], the recycle concentration factor [–] and the recycle ratio [–], respectively. These last two parameters are described in more detail in Section 3.2.

The rate of change of soluble micropollutants

$$V\frac{dC_s}{dt} = F(C_{s,\text{in}} - C_s) - HQ_{\text{air}}C_s - Vk_{\text{sor}}X_{\text{TSS}} \cdot C_s + V\frac{k_{\text{sor}}}{K_d} \cdot C_p - Vr_{\text{biol}}, \tag{3.3}$$

where the parameters $C_{s,\text{in}}$ and X_{TSS} are the concentration of soluble micropollutants in the feed [µg L^{-1}] and the total suspended solids [g SS L^{-1}], respectively.

The rate of change of particulates micropollutants

$$V\frac{dC_p}{dt} = F(C_{p,\text{in}} - C_p) + RF(C - 1)C_p + Vk_{\text{sor}}X_{\text{TSS}} \cdot C_s - V\frac{k_{\text{sor}}}{K_d}C_p, \tag{3.4}$$

where the parameter $C_{p,\text{in}}$ [µg L^{-1}] is the concentration of particulate micropollutants in the feed.

Monod growth kinetics

$$M_2(S_s) = \frac{S_s}{K_S + S_s}.$$

Residence time

$$\tau = \frac{V}{F},$$

where the parameter τ [day] is the residence time.

Biological removal rate ("linear" biodegradation model)

$$r_{\text{biol}} = k_{\text{biol}} \cdot X_{B,H} \cdot C_s. \tag{3.5}$$

Total suspended solids

$$X_{\text{TSS}} = c_2 X_{B,H},$$

TABLE 3. Typical parameter values. The parameters in the table are: $C_{s,\text{in}}$, the concentration of soluble micropollutants in the feed; K_S, the Monod constant for heterotrophic biomass; $S_{s,\text{in}}$, the substrate concentration in the feed; Y_H, the heterotrophic yield factor; b_H, the heterotrophic decay coefficient; c_2, a conversion factor from units of COD to units of TSS for the heterotrophic biomass; and μ_{max}, the maximum specific growth rate for biomass.

Parameter	Unit	Value	Reference
$C_{s,\text{in}}$	μg L^{-1}	100	Fernandez-Fontaina et al. [12]
K_S	g COD L^{-1}	0.020	Yoon and Lee [43]
$S_{s,\text{in}}$	g COD L^{-1}	0.2	Yoon and Lee [43]
Y_H	(g COD)(g COD)$^{-1}$	0.67	Yoon and Lee [43]
b_H	day^{-1}	0.22	Yoon and Lee [43]
c_2	g SS(g COD)$^{-1}$	0.90	Jeppsson and Diehl [19]
μ_{max}	day^{-1}	6.0	Yoon and Lee [43]

where the parameter c_2 converts units of chemical oxygen demand to units of total suspended solids [(g SS)/(g COD)]. The nomenclature is defined in Appendix A. In equations (3.1)–(3.4), the parameters that can be most easily manipulated experimentally are the specific aeration flow rate (Q_{air}), the concentration of soluble substrate in the feed ($S_{s,\text{in}}$) and the residence time (τ). The last of these is the main experimental control parameter.

The typical parameter values for the activated sludge process are taken from [43]. The typical parameter values for the variables associated with the micropollutants are taken from [12]. These values are presented in Tables 3 and 4, respectively. The micropollutants are classified into one of four groups depending upon their characteristics [12].

In Fernandez-Fontaina et al. [12, Table 3], the units of the parameter k_{biol} are L (g VSS day)$^{-1}$. We therefore required a conversion factor to convert these units to units of L (g COD day)$^{-1}$. This is given by [28, Ch. 2.2.4.1]

$$\text{COD} = f_x \text{VSS},$$

where $f_x = 1.42$ g cell COD/(g VSS).

In the following section, we discuss the settling unit model.

3.2. The ideal settling unit model In this section, we provide background information on settling units and our submodel for the settling unit: the ideal settling unit model, also known as the perfect or point settling unit model. The purpose of a settling unit, also known as a clarifier, secondary settling unit, sedimentation basin or solid–liquid separator, is to use the process of sedimentation under gravity to separate suspended solids, the biological sludge mass, from the liquid phase, the treated wastewater. Two important processes occurring within a settling unit are clarification and thickening. Clarification, which occurs in the upper zone of a settling unit, is the removal of finely dispersed solids from the liquid. This produces a low-turbidity

TABLE 4. Parameter values for the variables associated with the micropollutants. The average value of the two values reported in [12, Table 3] has been taken. The parameters in the table are: K_d, the solid–liquid partitioning coefficient; k_{biol}, the biotransformation kinetic constant; and k_{sor}, the sorption kinetic constant.

Type	k_{biol} L (g COD day)$^{-1}$	K_d L (g SS)$^{-1}$	k_{sor} (g SS)$^{-1}$
Highly biodegradable with low sorption	>1.42	$<100 \times 10^{-3}$	
Ibuprofen (IBP)	4.76	56.5×10^{-3}	96.0
Naproxen (NPX)	2.84	47.0×10^{-3}	129.5
Erythromycin (ERY)	2.70	59.5×10^{-3}	36.0
Roxithromycin (ROX)	4.05	89.5×10^{-3}	236.5
Highly biodegradable with high sorption	>1.42	$>100 \times 10^{-3}$	
Galaxolide (HHCB)	38.20	2704.5×10^{-3}	3036.5
Tonalide (AHTN)	21.23	2346×10^{-3}	1142.5
Slowly biodegradable	<1.42		
Fluoxetine (FLX)	1.35	902.5×10^{-3}	2074.5
Sulfamethoxazole (SMX)	0.92	48.0×10^{-3}	74.5
Trimethoprim (TMP)	0.64	75.5×10^{-3}	96.5
Nonbiodegradable	0		
Diclofenac (DCF)	0.00	$<5.5 \times 10^{-3}$	9.0
Carbamazepine (CBZ)	0.00	17.5×10^{-3}	43.5
Diazepam (DZP)	0.00	125.5×10^{-3}	122.5

effluent which is suitable for discharge into aquatic environments. Thickening, which occurs in the lower zone of a settling unit, is the concentration of sludge.

A settling unit has two output streams: the effluent stream, from the clarification zone, and the underflow stream, from the thickening zone. The former contains purified water which is low in suspended solids; ideally *free* of suspended solids. In our figure below this is the "top" stream with flow rate $(1 - w)F$. The latter contains settled concentrated biomass. This is either recycled back into the reactor, through the recycle stream, or sent for disposal, through the wastage stream.

Figure 1 shows the process configuration. The flow rate of the recycle stream from the settling unit, denoted F_R, is written as $F_R = RF$, where the parameter R is the recycle rate. The wastage rate from the settling unit, denoted F_W, is written as $F_W = wF$, where w is the fractional wastage. When a settling unit is deployed we have $R > 0$.

The thickening zone concentrates particulates. A common assumption in settling unit models is that all particulates are the same size and are concentrated equally by the
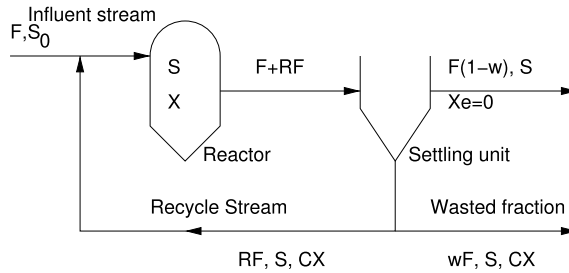
FIGURE 1. Schematic process configuration illustrating recycle and separate sludge wasting. C is the recycle concentration factor [–]. F is the flow rate through the bioreactor [L day^{-1}]. R is the recycle ratio [–]. S is the substrate concentration in the bioreactor [g COD L^{-1}]. S_0 is the substrate concentration in the feed [g COD L^{-1}]. X is the concentration of particulate biomass in the bioreactor [g COD L^{-1}]. X_e is the concentration of particulate biomass in the effluent stream [g COD L^{-1}]. w is the fraction of the recycle stream that is wasted [–].

settling unit. In the ideal settling unit model the concentration of particulates leaving the settling unit in the underflow is given by CP, where the parameter C is known as the concentration factor of the settling unit. Note that as the settling unit concentrates particulates, we must have $C > 1$. We have $P = X_{B,H}$ in equation (3.2) and $P = C_p$ in equation (3.4).

A mass balance around the settling unit reveals that the particulate concentration in the effluent stream is

$$P_e = \frac{1 - wC + R(1 - C)}{1 - w} \cdot P,$$

where P is the concentration in the stream leaving the bioreactor. A standard assumption is that the settling unit captures all particulates. Then $P_e = 0$, $C = C_{\max}$ and

$$[R(C_{\max} - 1)] = 1 - wC_{\max}.$$

This gives the maximum concentration factor

$$C_{\max} = \frac{1 + R}{R + w}.$$

The value of $C_{\max}$ is independent of the process load, only depending upon the recycle ratio (R) and the wastage fraction (w). As $0 \le w < 1$, the value of the maximum concentration factor is guaranteed to be greater than one.

It follows that when all the solids are captured,

$$R^* = R[C_{\max} - 1] = \frac{R(1 - w)}{R + w}.$$

The parameter grouping $R^* = R[C_{\max} - 1]$ is known as the effective recycle ratio. We have $0 \le R^* \le 1$. The maximum value ($R^* = 1$) can only be achieved if there is no wastage ($w = 0$). Thus, in practice, we have $0 \le R^* < 1$.

Although highly simplified, the point settler model is considered acceptable for conditions under which the flow rate and the total suspended solids in the influent stream of a WWTP are relatively constant [11]. It is useful when the main focus is on the overall behaviour of the system. Diehl et al. noted that "It is the most commonly used assumption for steady-state analysis in text books and papers" [10, Section 7]. However, when modelling dynamic conditions activated sludge models are mostly coupled with one-dimensional settling unit models [11].

3.3. Other models for the settling unit   The ideal settler unit model assumes a highly idealized operation of the settling unit. A key implicit assumption is that the settling unit is able to cope with *any* flux of particulate matter, that is, all the particulate matter entering the settling unit passes through the thickening zone and leaves in the underflow. However, in practice, settling units cannot be operated if the flux of particulate matter is over some maximum value; such a situation is known as overloading. Overloading, which may be due to reasons such as storm weather or settleability deterioration, may lead to process failure, for example, particulate matter may be discharged into the effluent stream. The phenomenon of overloading has motivated the design of improved models for settling units. In this section, we provide an overview of some relevant work over recent years. Our focus is on models that use solid flux theory. Other approaches are possible, for example, by considering the forces acting on settling particles [42].

Takács and Ekama [35] provided an excellent starting point to learn about settling units. They covered settling tank configurations, measures of sludge settleability, and provided an account of flux theory and how it is used to make the engineering calculations that are required for the design and operation of settling units. The section on the modelling of settlers divides post 1990 models into one-dimensional (1-D) models and computational fluid dynamics (CFD) models (2-D or 3-D). The former are more commonly used in conjunction with ASP models, whereas the latter are used in the design of settling units.

One-dimensional models describe the vertical sludge profile by discretizing the tank into horizontal layers, with uniform concentrations in each layer. This simplifies the hydrodynamic flow within the settling unit to be either "up", towards the effluent stream, or "down", towards the underflow. Three major zones are identified: the clarification zone, the inlet zone and the thickening zone. The clarification zone, at the top of the unit, sits above the inlet zone, which sits above the thickening zone, at the bottom of the unit. Many assumptions have to be made to reduce the complexity of the model. Standard assumptions include: the constituents of the suspension are incompressible; the stream from the biological reactor is completely flocculated before entering the settling unit; there is no mass transfer between the solid and liquid phases; and that no reactions occur in the settling unit. A fundamental problem in modelling settling units is that the various settling behaviours that can occur are poorly understood [22]. This has led to the widespread use of empirical or semi-empirical expressions for terms such as the settling velocity of particulate material.

The most common method describes the settling behaviour of particulates using a single concentration variable. Such models can be subdivided into first-order and second-order models, also referred to as convection and convection–diffusion models, respectively. First-order (convection) models are based upon mass continuity and give rise to a nonlinear hyperbolic partial differential equation (PDE). Two mechanisms are used to model the continuity of solids flux: hindered settling due to gravity and bulk transport due to upwards and downwards hydraulic flow. Most early one-dimensional models only considered conservation of mass and hindered settling [24, p. 235].

In second-order (convection–diffusion) models, a diffusion term is included in an attempt to incorporate hydrodynamic features. This gives a nonlinear parabolic PDE. An advantage of second-order models is that there is a clear distinction between settling parameters, which can be measured, and "lumped parameters", which lump together hydrodynamic effects, which are adjusted during the process of model calibration [11, 31].

At low concentrations, suspended particles are subject to hindered settling. At high concentrations, particles are instead subject to compression settling. This occurs due to the transmission of compressive stress as a consequence of the formation of a (compressible) porous layer of flocculated particles. Although conceptually simple, the constitutive relationships describing compressive behaviour are still unknown [38]. The interface between the region of hindered settling and compression settling is known as the sludge blanket. A major complication in modelling compression is that the location of the sludge blanket is not static. Under conditions of overloading, the sludge blanket can move from the "bottom" of the settling unit to its "top", resulting in process failure due to the discharge of suspended solids into the effluent stream. The earliest, and simplest, one-dimensional models did not include compressive settling.

The one-dimensional modelling of secondary settling tanks has been reviewed by Li and Stenstrom [22] and by Cadet et al. [5]. Li and Stenstrom's review divides into three main parts: settling theory, one-dimensional models and suitable numerical techniques. In their complementary review, Cadet et al. explored the defects in one-dimensional models. These are primarily identified as being a lack of knowledge about the fundamental physical processes occurring within a settling unit and the difficulties in numerically solving the resulting PDE models. A complete CFD simulation of the complicated multiphase fluid motion within a settling tank is currently not feasible due to the wide range of physico-biochemical phenomena occurring inside it and a lack of understanding about the settling characteristics of sludge [21, Section 6.1].

The most widely used one-dimensional settling tank model in WWTP modelling is the first-order model due to Takács et al. [36]. This model has been found to work best with 10 layers comprising: the top layer, corresponding to the effluent stream, three clarifier layers, the feed layer, four thickening layers and the bottom layer, corresponding to the underflow stream. For an applied mathematician, a worrying feature of the Takács model is that, as the number of layers is increased, its solution fails to converge to the solution of the underlying PDE [18]. Furthermore, increasing the number of layers deteriorates the fit of the model to experimental data [41].

One reason for such behaviour is that the discretized model includes a parameter, a threshold concentration, which is not present in the PDE model. Despite its defects, this model can provide reasonable predictions for settling units running under normal operating conditions, that is, normal dry weather. It has been "implemented in most commercial simulators as a reference model" [23, p. 814]. However, it is not recommended to use it under anomalous operating conditions such as peak flows due to rain [37].

A one-dimensional model that includes compressive settling is the hindered-compression–dispersion model due to Bürger and Diehl, the Bürger–Diehl model. At the time of its publication, it was the most advanced one-dimensional settling tank model [23]. The potential advantages of this model include its ability to provide more accurate predictions of underflow concentrations and to determine the location of the sludge blanket under unusual conditions [24].

Torfs et al. [37] coupled the Bürger–Diehl settling unit model to the benchmark simulation model no. 1 (BSM1) [2], a standard model for a WWTP. The authors' aim was not to investigate a fully calibrated model, rather it was to identify circumstances under which the Bürger–Diehl model captures dynamic features of the settling unit that were not captured by traditional models. The simulations used a standard input file for storm weather conditions.

Li and Stenstrom [23] provided a sensitivity analysis of the Bürger–Diehl model under wet-weather flow and sludge bulking conditions. The modelling platform used was the BSM1 [2]. The authors found that the relative importance of the parameters in the settling unit model depended upon the imposed simulation conditions.

Diehl et al. [9] investigated the steady-state behaviour of a bioreactor connected to a settling unit, the latter using the Bürger–Diehl model. The biological processes were represented by one reaction: the growth of a single biomass species upon one substrate. For their steady-state analysis, the authors assumed that *all* the sludge entering the settling unit moves through the thickening zone and that there is no sludge in the effluent stream, that is, the settling unit can never be overloaded. To ensure that this was the case, the recycle ratio (R) and the wastage ratio (w) unit were varied in order to ensure that the location of the sludge blanket remained level at 1 m.

Diehl et al. [9] modelled the bioreactor as a continuously stirred tank reactor. In a complementary study, the bioreactor was instead assumed to be a plug-flow reactor [10]. As before, the authors assumed that the reactor cannot be overloaded and varied the recycle ratio and the wastage ratio to ensure that the location of the sludge blanket remains fixed at 1 m. One point of difference is that the steady-state solutions obtained using the Bürger–Diehl settling tank model were compared to those using the ideal settling tank model.

A standard assumption is that no reactions occur in settling units. However, significant denitrification can occur at the bottom of settling tanks. Bürger et al. [3] extended the Bürger–Diehl model to include biochemical reactions. A kinetic model was used containing five state variables, three soluble species and two particulates. This led to a system of nonlinear convection–diffusion–reaction PDEs, which had to

be solved using a nonstandard numerical method. The model was solved within the context of batch settling; it was linked to a model for a WWTP.

A practical obstacle to the use of advanced models for settling units is the paucity of high-resolution data sets. Well-collected data sets from batch tests are required to calibrate the empirical functions that are ubiquitous in settling unit models. Such tests are labour intensive and typically information poor [24, Section 2.2]. Well-collected data sets from WWTPs are required for model validation and comparison. The limited observational data, of both types, has ensured that many settling tank models have not been verified and tested [22]. Even when batch data is available, the observational data is limited, which means that it is difficult to find a unique set of model parameter values. The selection of *initial* guesses for parameters associated with biomass settleability and compressibility can be challenging due to insufficient knowledge as to what "typical" values might be [24, Section 2.3]. These problems have limited the practical applications of advanced settler models, such as the Bürger–Diehl model [23]. The problems associated with parameter identification are exacerbated in advanced settler models due to the additional parameters that they contain compared to traditional models. For example, the Bürger–Diehl model contains additional parameters associated with compressive setting. More recent settling unit models contain close to 10 parameters [24, Section 4]. Motivated by such concerns, the sensitivity of model predictions to both to the choice of settling unit models and the uncertainty in the values of settling unit parameters has been investigated [24, 31].

Ramin et al. [31] used global sensitivity techniques to investigate how the choice of settling tank model and the uncertainty in the settling unit model parameters affect the performance of WWTP models. First-order and second-order one-dimensional settling unit models were used. Dynamic simulations were carried out with daily, weekly and seasonal variation in both dry- and wet-weather conditions. The uncertainty in the settling unit parameters was found to be as influential as the uncertainty in the biokinetic parameters of the activated sludge model no. 1. Furthermore, the relative importance of the settling unit parameters depended upon which submodel was being considered.

The problem of parameter identifiability in the Bürger–Diehl model without dispersion was considered by Li and Stenstrom [24]. They investigated which settling unit parameters can be identified from which experimental configurations, the influence of the initial guess for the parameter values upon parameter identifiability and how differences in parameter estimates impact the uncertainty in the prediction of a model.

The one-dimensional models discussed above describe the behaviour of the particulates through a single concentration variable. This implies that all the particulates are the same size. Torfs et al. [38] have extended the Bürger–Diehl model to include the size distribution of particles. Not only do the different particle classes have different settleability characteristics, but the model contains "reaction" terms allowing flocculation of smaller particles to produce larger particles and for larger

particles to break apart into smaller ones. The model equations were implemented as a batch sedimentation model containing 10 particle classes; they were not attached to a WWTP model.

An alternative approach to the use of single-phase models are two-phase models in which both solid and liquid concentrations are modelled. The use of both mass continuity and conservation of momentum leads to a system of four PDEs, two for each phase. Such models provide a more detailed description of physical processes, in particular those associated with the compression zone. However, this greater detail comes at the expense of introducing more processes which must be parameterized. Such models have been reviewed by Li and Stenstrom [22].

4. Biological removal: a linear biodegradation model

4.1. The dimensionless model In this section, we study the system (3.1)–(3.4) associated with the linear biotransformation rate defined by equation (3.5). The model equations (3.1)–(3.4) are scaled using the dimensionless variables: $[S^* = S_s/K_S]$, $[X^* = X_{B,H}/Y_H K_S]$, $[C_s^* = C_s/C_{s,\text{in}}]$, $[C_p^* = C_p/C_{s,\text{in}}]$ and $[t^* = \mu_{\max} t]$. This process introduces: scaled feed concentrations $[C_{p,\text{in}}^* = C_{p,\text{in}}/C_{s,\text{in}}$, $S_{s,\text{in}}^* = S_{s,\text{in}}/K_S$, $X_0^* = X_0/(Y_K S_s)]$, a scaled solid–liquid partitioning coefficient $[K_d^* = c_2 K_S Y_H \cdot K_d]$, a scaled specific aeration rate $[Q_{\text{eff}} = H Q_{\text{air}}/(V \mu_{\max,H})]$, an effective recycle ratio $[R^* = (C - 1)R]$, a scaled decay rate $[b_H^* = b_H/\mu_{\max,H}]$, a scaled biotransformation kinetic constant $[k_{\text{biol}}^* = K_S Y_H \cdot k_{\text{biol}}/\mu_{\max,H}]$, a scaled sorption rate $[k_{\text{sor}}^* = c_2 K_S Y_H \cdot k_{\text{sor}}/\mu_{\max,H}]$ and a scaled residence time $[\tau^* = \tau \cdot \mu_{\max,H}]$. The system of scaled equations is

$$\frac{dS^*}{dt^*} = \frac{S_{s,\text{in}}^* - S^*}{\tau^*} - \frac{X^* S^*}{1 + S^*}, \tag{4.1}$$

$$\frac{dX^*}{dt^*} = \frac{X_0^* - X^*}{\tau^*} + \frac{X^* S^*}{1 + S^*} - b_H^* X^* + \frac{R^* X^*}{\tau^*}, \tag{4.2}$$

$$\frac{dC_s^*}{dt^*} = \frac{1 - C_s^*}{\tau^*} - Q_{\text{eff}} C_s^* - k_{\text{sor}}^* C_s^* X^* + \frac{k_{\text{sor}}^*}{K_d^*} C_p^* - k_{\text{biol}}^* X^* C_s^*, \tag{4.3}$$

$$\frac{dC_p^*}{dt^*} = \frac{C_{p,\text{in}}^* - C_p^*}{\tau^*} + \frac{R^* C_p^*}{\tau^*} + k_{\text{sor}}^* C_s^* X^* - \frac{k_{\text{sor}}^*}{K_d^*} C_p^*. \tag{4.4}$$

From now on, we assume that the particulate biomass and the particulate micropollutant concentrations in the feed are zero ($X_0^* = 0$ and $C_{p,\text{in}}^* = 0$). Several authors have reported that stripping, that is, mass transfer into the gas phase, is negligible [1, 12, 20, 39]. In any case, stripping could only be significant for volatile micropollutants. Urase and Kikuta [39] provided a bound on the value of Henry's constant, below which it can be assumed that transfer of compounds to the air phase is negligible. Some models do not contain a mass transfer term as it is assumed that biological removal and sorption are much more important that volatilization. Examples of this are models for the removal of pentachlorophenol [17] and nitrilotriacetate [32]. In view of the considerations outlined above, we remove the specific aeration term from our model, that is, $Q_{\text{eff}} = 0$.

4.2. Steady-state solutions   There are two branches of steady-state solutions. The first of these is the washout branch,

$$(S^*, X^*, C_s^*, C_p^*) = (S_{s,\text{in}}^*, 0, 1, 0).$$

This is so-named because the bioreactor is devoid of biomass ($X^* = 0$). The second of these is the no-washout branch

$$(S^*, X^*, C_s^*, C_p^*) = \left(\widehat{S^*}, \frac{S_{s,\text{in}}^* - \widehat{S^*}}{1 - R^* + b_H^*\tau^*}, d_1\left[1 - R^* + \tau^*\frac{k_{\text{sor}}^*}{K_d^*}\right], d_1\,\tau^* k_{\text{sor}}^* X^*\right),$$

$$\widehat{S^*} = \frac{1 - R^* + b_H^*\tau^*}{(1 - b_H^*)\tau^* - (1 - R^*)},$$

$$d_1 = \frac{1}{[(k_{\text{sor}}^*/K_d^*)\,d_2 + (1 - R^*)k_{\text{sor}}^* X^*]\tau^* + d_2(1 - R^*)},$$

$$d_2 = 1 + k_{\text{biol}}^* X^*\tau^*.$$

This is so-named because the bioreactor contains biomass ($X^* > 0$). Note that we have $d_1 > 0$ and $d_2 > 0$.

The no-washout branch is only of interest when the components are positive ($0 < S_s^* < S_{s,\text{in}}^*, X^* > 0, C_s^* > 0, C_p^* > 0$). These conditions are met if the dimensionless residence time is sufficiently high and the dimensionless decay rate is sufficiently low,

$$\tau^* > \tau_{\text{cr}}^* = \frac{(1 + S_{s,\text{in}}^*)(1 - R^*)}{S_{s,\text{in}}^* - (1 + S_{s,\text{in}}^*)b_H^*} > 0,$$

$$0 < b_H^* < \frac{S_{s,\text{in}}^*}{1 + S_{s,\text{in}}^*}. \tag{4.5}$$

(Recall from Section 3.2 that we have $0 \le R^* \le 1$.)

A transcritical bifurcation occurs when $\tau^* = \tau_{\text{cr}}^*$. At this point, the no-washout and washout solution branches intersect. Note that this critical value approaches zero as the value of the effective recycle parameter approaches its theoretical maximum ($R^* = 1$). The use of a settling unit allows the reactor to operate at lower residence times.

The dimensionless soluble micropollutant concentration and the dimensionless particulate micropollutant concentration are both decreasing functions of the dimensionless biotransformation kinetic constant (k_{biol}^*). Differentiating the steady-state equations (4.3) and (4.4) with respect to k_{biol}^*,

$$\frac{dC_p^*}{dk_{\text{biol}}^*} = \frac{-k_{\text{sor}}^* X^{*2}\tau^{*2}C_s^*}{[X^*\tau^*(k_{\text{sor}}^* + k_{\text{biol}}^*) + 1][1 - R^*]K_d^* + k_{\text{sor}}^*\tau^*[k_{\text{biol}}^* X^*\tau^* + 1]} < 0,$$

$$\frac{dC_s^*}{dk_{\text{biol}}^*} = \frac{-X^* C_s^*\tau^*[(1 - R^*)K_d^* + k_{\text{sor}}^*\tau^*]}{[X^*\tau^*(k_{\text{sor}}^* + k_{\text{biol}}^*) + 1][1 - R^*]K_d^* + k_{\text{sor}}^*\tau^*[k_{\text{biol}}^* X^*\tau^* + 1]} < 0. \tag{4.6}$$

(Prior to differentiating equations (4.3) and (4.4), it is useful to note that the steady-state expressions for the substrate and biomass concentrations, S^* and X^*, respectively,

are independent of the parameter k^*_{biol}.) Hence, these concentrations decrease as the dimensionless biotransformation kinetic constant increases. As the value of the dimensionless biotransformation kinetic constant (k^*_{biol}) increases, the dimensionless soluble micropollutant is more rapidly removed by the biomass. The removal of soluble micropollutant induces more particulate micropollutant to be desorbed.

The soluble micropollutant concentration and the particulate micropollutant concentration are decreasing and increasing as functions of the dimensionless solid–liquid partitioning coefficient (K^*_d), respectively. Differentiating the steady-state equations (4.3) and (4.4) with respect to K^*_d,

$$\frac{dC^*_p}{dK^*_d} = \frac{(k^*_{\text{sor}}\tau^*)^2 X^* d_2}{[(1-R^*)K^*_d X^* k^*_{\text{sor}}\tau^* + d_2\{k^*_{\text{sor}}\tau^* + (1-R^*)K^*_d\}]^2},$$

$$\frac{dC^*_s}{dK^*_d} = \frac{-(1-R^*)(k^*_{\text{sor}}\tau^*)^2 X^*}{[(1-R^*)K^*_d X^* k^*_{\text{sor}}\tau^* + d_2\{k^*_{\text{sor}}\tau^* + (1-R^*)K^*_d\}]^2}.$$

(Before carrying out the implicit differentiation, it should be noted that the steady-state expressions for the substrate and biomass concentrations are independent of the parameter K^*_d.) In our model formulation, increasing the dimensionless solid–liquid partitioning coefficient corresponds to decreasing the rate of the desorption. It is therefore to be expected that this acts to increase the particulate micropollutant concentration at the expense of the soluble micropollutant concentration. We conclude that the soluble micropollutant concentration is minimized by taking high values for k^*_{biol} and K^*_d.

4.3. Local stability The local stability of the steady-state solutions is governed by the eigenvalues of the Jacobian matrix of the model (4.1)–(4.4). We have

$$J(S^*, X^*, C^*_s, C^*_p) = \begin{bmatrix} -A_1 & -A_2 & 0 & 0 \\ A_3 & A_4 & 0 & 0 \\ 0 & -A_5 & -A_6 & A_7 \\ 0 & A_8 & A_9 & -A_{10} \end{bmatrix}, \tag{4.7}$$

where

$$A_1 = \frac{1}{\tau^*} + \frac{X^*}{(1+S^*)^2}, \quad A_2 = \frac{S^*}{(1+S^*)}, \quad A_3 = \frac{X^*}{(1+S^*)^2},$$

$$A_4 = \frac{R^* - 1 - b^*_H\tau^*}{\tau^*} + \frac{S^*}{1+S^*}, \quad A_5 = (k^*_{\text{sor}} + k^*_{\text{biol}})\, C^*_s, \quad A_6 = \frac{1}{\tau^*} + X^*[k^*_{\text{sor}} + k^*_{\text{biol}}],$$

$$A_7 = \frac{k^*_{\text{sor}}}{K^*_d}, \quad A_8 = k^*_{\text{sor}}\, C^*_s, \quad A_9 = k^*_{\text{sor}}X^*, \quad A_{10} = \frac{1-R^*}{\tau^*} + \frac{k^*_{\text{sor}}}{K^*_d}.$$

4.3.1 *Stability of the washout solution branch.* Along the washout solution branch, the eigenvalues of the Jacobian matrix are given by

$$\lambda_{1,2} = -\frac{1}{\tau^*} < 0,$$

$$\lambda_3 = \frac{R^* - 1 - (k^*_{\text{sor}}/K^*_d)\tau^*}{\tau^*} < 0,$$

$$\lambda_4 = \frac{R^* - 1 - b^*_H \tau^*}{\tau^*} + \frac{S^*_{s,\text{in}}}{1 + S^*_{s,\text{in}}}.$$

Note that $0 \leq R^* < 1$. Rearranging the expression for λ_4, we find that the eigenvalue is negative when

$$[S^*_{s,\text{in}} - b^*_H(1 + S^*_0)]\tau^* < (1 - R^*)(1 + S^*_{s,\text{in}}).$$

This shows that the eigenvalue is always negative when the decay rate is sufficiently high, that is,

$$b_H \geq \frac{S^*_{s,\text{in}}}{1 + S^*_{s,\text{in}}}.$$

When this inequality does not hold, that is,

$$b_H < \frac{S^*_{s,\text{in}}}{1 + S^*_{s,\text{in}}},$$

the washout steady-state solution is stable if the dimensionless residence time is sufficiently low:

$$\tau^* < \tau^*_{\text{cr}} = \frac{(1 + S^*_{s,\text{in}})(1 - R^*)}{S^*_{s,\text{in}} - (1 + S^*_{s,\text{in}})b^*_H}.$$

Using standard methods [27], it can be shown that the washout solution branch is globally stable if it is locally stable.

4.3.2 *Stability of the no-washout solution branch.* For *any* steady-state solution, we have from equation (4.2) that

$$0 = X^*\left(\frac{R^* - 1}{\tau^*} + \frac{S^*}{1 + S^*} - b^*_H\right).$$

The washout branch corresponds to the solution $0 = X^*$, whereas the no-washout branch corresponds to the solution

$$0 = \frac{R^* - 1}{\tau^*} + \frac{S^*}{1 + S^*} - b^*_H.$$

Observe that the expression at $J_{2,2}$ is exactly

$$J_{2,2} = \frac{R^* - 1}{\tau^*} + \frac{S^*}{1 + S^*} - b^*_H.$$

It immediately follows that along the no-washout solution branch we have $J_{2,2} = 0$.

Along this solution branch, the characteristic polynomial of the Jacobian matrix (4.7) is given by

$$C(\lambda) = [\lambda^2 + a_1\lambda + a_2][\lambda^2 + A_1\lambda + A_3A_2], \tag{4.8}$$
$$a_1 = A_6 + A_{10},$$
$$a_2 = A_6A_{10} - A_7A_9.$$

This solution branch is only of interest when the solution components are all positive. Under these circumstances, the coefficients in the Jacobian matrix, A_i, $i = 1, \ldots, 10$, are also positive.

Equation (4.8) is a product of two quadratic equations. The conditions for the steady-state solution to be locally stable are: $a_1 > 0$, $a_2 > 0$, $A_1 > 0$ and $A_3A_2 > 0$. The coefficients a_1, A_3A_2 and A_1 are immediately seen to be positive. To prove that $a_2 > 0$,

$$a_2 = A_6A_{10} - A_7A_9 = \frac{A_{10} + X^*\tau^*(k_{\text{sor}}^*/K_d^*)k_{\text{biol}}^* + X^*[k_{\text{sor}}^* + k_{\text{biol}}^*][1 - R^*]}{\tau^*} > 0.$$

We conclude that when the no-washout branch is physically meaningful, it is stable.

4.4. Asymptotic solution along the no-washout solution branch

At large values of the dimensionless residence time, the solution components along the no-washout solution branch are approximated by

$$S^* \approx \frac{b_H^*}{1 - b_H^*} + \frac{1 - R^*}{(1 - b_H^*)^2} \cdot \frac{1}{\tau^*} + O\left(\frac{1}{\tau^{*2}}\right), \tag{4.9}$$

$$X^* \approx \frac{S_{s,\text{in}}^* - b_H^*(S_{s,\text{in}}^* + 1)}{b_H^*(1 - b_H^*)} \cdot \frac{1}{\tau^*} + O\left(\frac{1}{\tau^{*2}}\right), \tag{4.10}$$

$$C_s^* \approx \frac{b_H^*(1 - b_H^*)}{[S_{s,\text{in}}^* - b_H^*(S_{s,\text{in}}^* + 1)]k_{\text{biol}}^* + b_H^*(1 - b_H^*)} - \frac{(1 - R^*)[K_d^*C_1 - k_{\text{biol}}^*C_2]}{C_3^2} \cdot \frac{1}{\tau^*}$$
$$+ O\left(\frac{1}{\tau^{*2}}\right), \tag{4.11}$$

$$C_p^* \approx \frac{K_d^*[S_{s,\text{in}}^* - b_H^*(S_{s,\text{in}}^* + 1)]}{k_{\text{sor}}^*[(S_{s,\text{in}}^* - b_H^*(S_{s,\text{in}}^* + 1))k_{\text{biol}}^* + b_H^*(1 - b_H^*)]} \cdot \frac{1}{\tau^*} + O\left(\frac{1}{\tau^{*2}}\right), \tag{4.12}$$

$$C_1 = b_H^*(1 - b_H^*)[S_{s,\text{in}}^* - b_H^*(1 + S_{s,\text{in}}^*)] > 0,$$
$$C_2 = (1 - b_H^*)^2 S_{s,\text{in}}^* + b_H^{*2} > 0,$$
$$C_3 = -k_{\text{biol}}^*(1 - b_H^*)S_{s,\text{in}}^* - b_H^*(1 - b_H^* - k_{\text{biol}}^*).$$

Note that from equation (4.5), this solution branch is only meaningful when $b_H^* < [S_{s,\text{in}}^*/(1 + S_{s,\text{in}}^*)]$. Thus, $[S_{s,\text{in}}^* - b_H^*(1 + S_{s,\text{in}}^*)] > 0$. Equations (4.9) and (4.11) show that the dimensionless effluent concentration and the dimensionless soluble

micropollutant concentration reach limiting value at large dimensionless residence times,

$$\lim_{\tau^* \to +\infty} S^* = \frac{b_H^*}{1 - b_H^*} > 0,$$

$$\lim_{\tau^* \to +\infty} C_s^* = \frac{b_H^*(1 - b_H^*)}{[S_{s,\text{in}}^* - b_H^*(S_{s,\text{in}}^* + 1)]k_{\text{biol}}^* + b_H^*(1 - b_H^*)} > 0. \tag{4.13}$$

These limiting concentrations are independent of the values associated with the adsorption (k_{sor}^*) and desorption (K_d^*) processes.

From equation (4.13), note that when there is no biological reaction ($k_{\text{biol}}^* = 0$), the limiting value of the dimensionless soluble micropollutant concentration is equal to the dimensionless influent concentration,

$$\lim_{\tau^* \to +\infty} C_s^*(k_{\text{biol}}^* = 0) = 1.$$

The reason for this is: when $k_{\text{biol}}^* = 0$, there is no biological removal of the micropollutant. The only removal mechanism for the micropollutant is through adsorption onto the microorganisms. However, in the limit of the large residence times, equation (4.10) shows that the microorganism concentration approaches zero. Consequently, there are no microorganisms to be absorbed onto.

When the micropollutant is not biodegradable, the concentration of soluble micropollutants along the no-washout branch simplifies to

$$C_s^*(\tau^*) = \frac{1 - R^* + k_{\text{sor}}^* \tau^*/K_d^*}{1 - R^* + k_{\text{sor}}^* \tau^*/K_d^* + (1 - R^*)k_{\text{sor}}^* X(\tau^*)\tau^*}, \quad \tau_{\text{cr}}^* \leq \tau^*.$$

This is a continuous function with value $C_s^* = 1$ when $\tau^* = \tau_{\text{cr}}^*$ and limiting value $\lim_{\tau^* \to \infty} C_s^* = 1$. As $C_s^* < 1$ for $\tau_{\text{cr}}^* < \tau^* < \infty$, we conclude that, when the micropollutant is nonbiodegradable, there must be a finite value of the dimensionless residence which minimizes its value. This is an interesting finding that has not been reported previously.

Note from equation (4.11) that if the term $(K_d^* C_1 - k_{\text{biol}}^* C_2)$ is positive (negative), then the soluble micropollutant concentration increases (decreases) to its limiting value. This shows that in the former case the concentration of soluble micropollutant is minimized at a finite residence time. This case happens when

$$\frac{K_d^*}{k_{\text{biol}}^*} > \frac{(1 - b_H^*)^2 S_{s,\text{in}}^* + b_H^{*2}}{b_H^*(1 - b_H^*)[S_{s,\text{in}}^* - b_H^*(1 + S_{s,\text{in}}^*)]}. \tag{4.14}$$

This behaviour cannot occur in the limit $b_H^* = 0$.

The right-hand side of inequality (4.14) only depends upon the values of $S_{s,\text{in}}^*$ and b_H^*. Using the parameter values in Table 3, we find that the right-hand side is equal to 27.38089632. In Table 7, we calculate the left-hand side of the inequality (4.14) for each of the 11 micropollutants. We observe that only nonbiodegradable micropollutants (CBZ and DZP) satisfy inequality (4.14) and thus these are the only micropollutants that increase to their limiting values.

Equations (4.10) and (4.12) show that both the dimensionless microorganism concentration and the dimensionless particulate micropollutant concentration decrease to zero.

We note that the limiting value of all solution components is independent of the effective recycle ratio (R^*). In equations (4.9)–(4.12), the recycle ratio only influences, as a second-order effect, the concentrations of the soluble substrate and the soluble micropollutant. When the micropollutant is not biodegradable ($k^*_{\text{biol}} = 0$), we have from equation (4.11) that

$$\frac{dC^*_s}{dR^*}\bigg|_{k^*_{\text{biol}}=0} = \frac{S^*_{s,\text{in}} - b^*_H(1 + S^*_{s,\text{in}})}{b^*_H \tau^*(1 - b^*_H)} \cdot K^*_d \cdot \frac{1}{\tau^*} > 0. \tag{4.15}$$

This shows that when the micropollutant is not biodegradable that recycle increases the concentration of soluble micropollutants at large residence times.

4.5. Steady-state diagrams: no settling unit In this section, we investigate steady-state diagrams when there is no settling unit ($R = R^* = 0$). Although this is not realistic from the perspective of an ASP plant, it does model another treatment method: the aerated lagoon. In any case, this section provides a baseline for evaluating the effect of recycle.

Steady-state diagrams for 11 micropollutants are shown in Figure 2. It is assumed that there is no recycle. The micropollutants considered are those investigated in [12]. These compounds represent four possible types of micropollutant behaviour [12]. These are (i) highly biodegradable with low sorption; (ii) highly biodegradable with high sorption; (iii) slowly biodegradable; and (iv) nonbiodegradable.

The soluble micropollutant concentration is equal to one along the washout branch ($\tau^* < \tau^*_{\text{cr}} = 1.146$). After the transcritical bifurcation, the concentration of soluble micropollutants initially decreases. At sufficiently high residence times it may increase to its limiting value. This depends upon the sign of the coefficient of the term τ^* in equation (4.11). For nonbiodegradable compounds, equation (4.15) shows that the soluble micropollutant decreases to the minimum point before increasing to its asymptotic value.

From equation (4.11), note that the concentration of soluble micropollutants approaches the limiting value

$$\lim_{\tau^* \to +\infty} C^*_s = \begin{cases} \dfrac{b^*_H(1 - b^*_H)}{[S^*_{s,\text{in}} - b^*_H(S^*_{s,\text{in}} + 1)]k^*_{\text{biol}} + b^*_H(1 - b^*_H)}, & k^*_{\text{biol}} > 0, \\ 1, & k^*_{\text{biol}} = 0. \end{cases}$$

Figure 2(d) shows, as noted in Section 4.4, that if the micropollutant is nonbiodegradable then the soluble micropollutant concentration approaches the value in the influent at large residence times. The limiting value of the soluble micropollutant concentration for all compounds is presented in Table 5. The limiting soluble micropollutant concentration is only influenced by one parameter associated with the micropollutants (k^*_{biol}) and two parameters associated with activated sludge (b^*_H

(a) Highly biodegradable with low sorption

(b) Highly biodegradable with high sorption

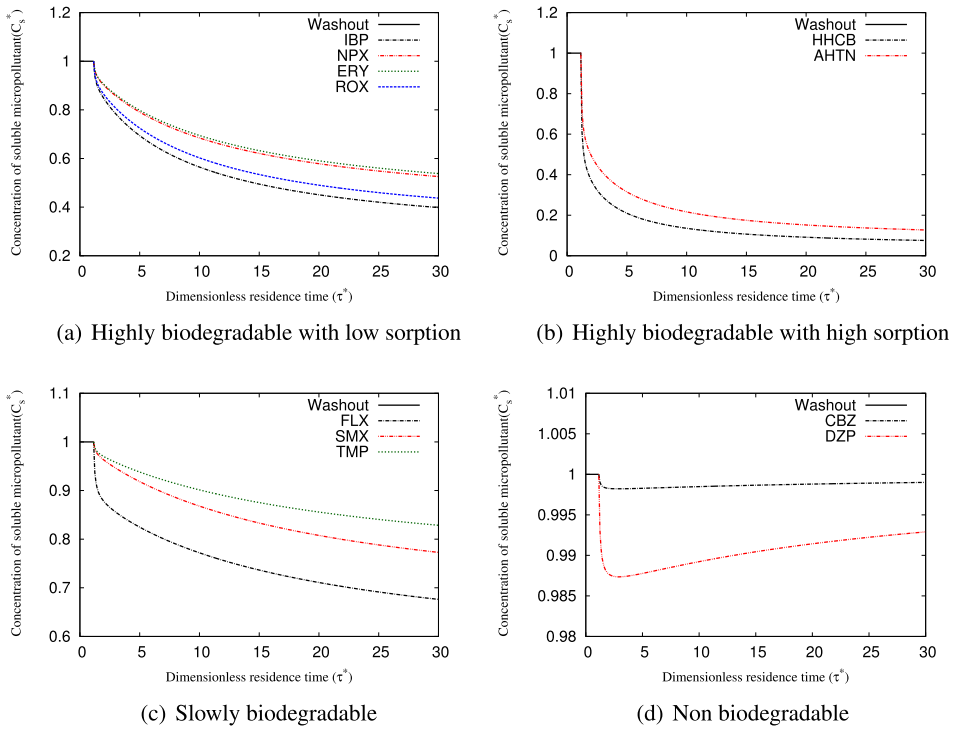(c) Slowly biodegradable

(d) Non biodegradable

FIGURE 2. Steady-state diagrams for the dimensionless soluble micropollutant concentration when there is no settling unit ($R^* = 0$) (colour available online). In (d) the concentrations of CBZ and DZP are minimized at dimensionless residence times $\tau^* = 2.91$ and $\tau^* = 2.92$, respectively. The washout line corresponds to process failure as there is no active biomass in the bioreactor ($X^* = 0$). Parameter values stated in Tables 3 and 4.

and $S^*_{s,\text{in}}$). Note that the limiting soluble micropollutant concentration can be decreased by increasing the influent substrate concentration ($S^*_{s,\text{in}}$).

From equation (4.6), we know that as the biotransformation kinetic constant (k_{biol}) increases, the concentration of soluble micropollutant decreases. Suppose that we specify a desired maximum concentration of the micropollutant in the effluent ($0 < C^*_{s,e} < 1$). Then, at high residence times, equation (4.11) gives the requirement that

$$k^*_{\text{biol}} > \frac{b^*_H(1 - C^*_{s,e})(1 - b^*_H)}{C^*_{s,e}[S^*_{s,\text{in}} - b^*_H(S^*_{s,\text{in}} + 1)]}.$$

In practice, it may not be possible to increase the value for the biotransformation constant k^*_{biol}. However, increasing the substrate concentration in the feed has an equivalent effect.

Figure 2(b) shows that the removal of the micropollutant is optimized when it is highly biodegradable with high sorption, while the removal of the micropollutant decreases if it is slowly biodegradable, as in Figure 2(c). Figure 2(d) demonstrates

(a) Highly biodegradable with low sorption

(b) Highly biodegradable with high sorption

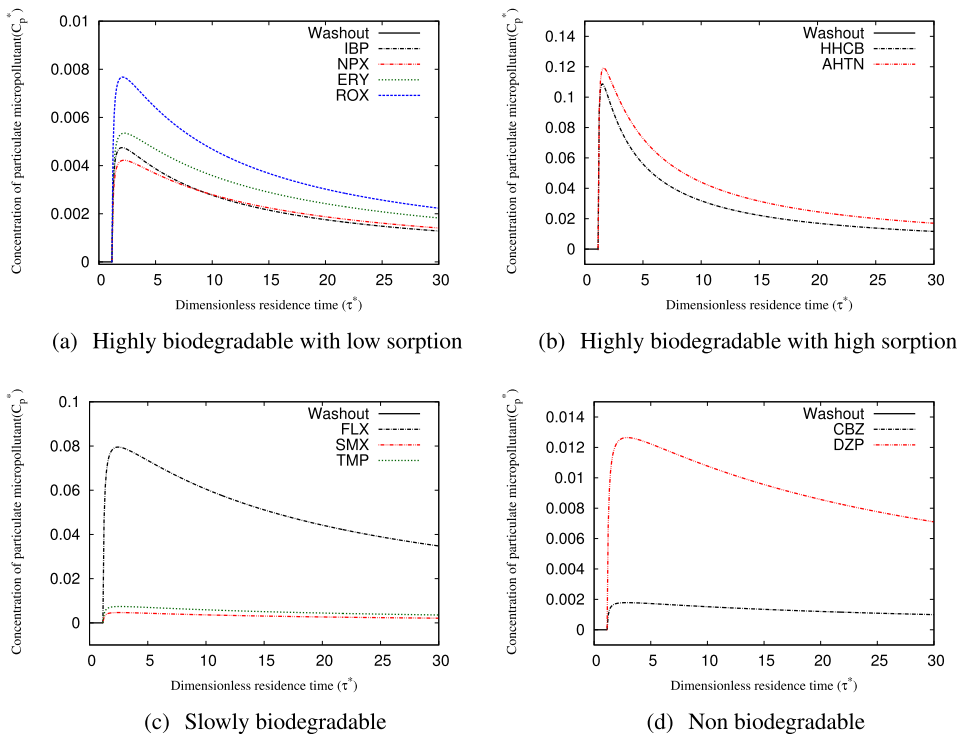(c) Slowly biodegradable

(d) Non biodegradable

FIGURE 3. Steady-state diagrams for the dimensionless particulate micropollutant concentration when there is no settling unit ($R^* = 0$) (colour available online). The washout line corresponds to process failure as there is no active biomass in the bioreactor ($X^* = 0$). Parameter values stated in Tables 3 and 4.

that when the micropollutant is not biodegradable, its concentration is minimized at a finite value of the residence time. At this point, the removal of CBZ and DZP are 0.1785% and 1.265%, respectively. Thus, there is an insignificant removal of these nonbiodegradable compounds.

Figure 3 shows the steady-state particulate micropollutant concentration when there is no recycle. Along the no-washout branch, the concentration increases sharply from its initial zero value to reach a maximum value. These maximum values are shown in Table 5. After the maximum value, the concentration decreases towards a limiting value, given by equation (4.12) when the residence time approaches infinity.

For a nonbiodegradable micropollutant shown in Figure 3(d), the maximum particulate micropollutant concentration is very low. This accounts for the negligible removal of soluble micropollutant shown in Figure 2(d).

4.6. Steady-state diagrams: the effect of recycle   We now investigate how the particulate micropollutant concentration and the soluble micropollutant concentration change in response to the deployment of a settling unit. We pick one example of each of the four classes of micropollutants: IBP, HHCB, FLX and DZP. We show that when

(a) Highly biodegradable with low sorption (IBP)

(b) Highly biodegradable and sorption (HHCB)

(c) Slowly biodegradable (FLX)
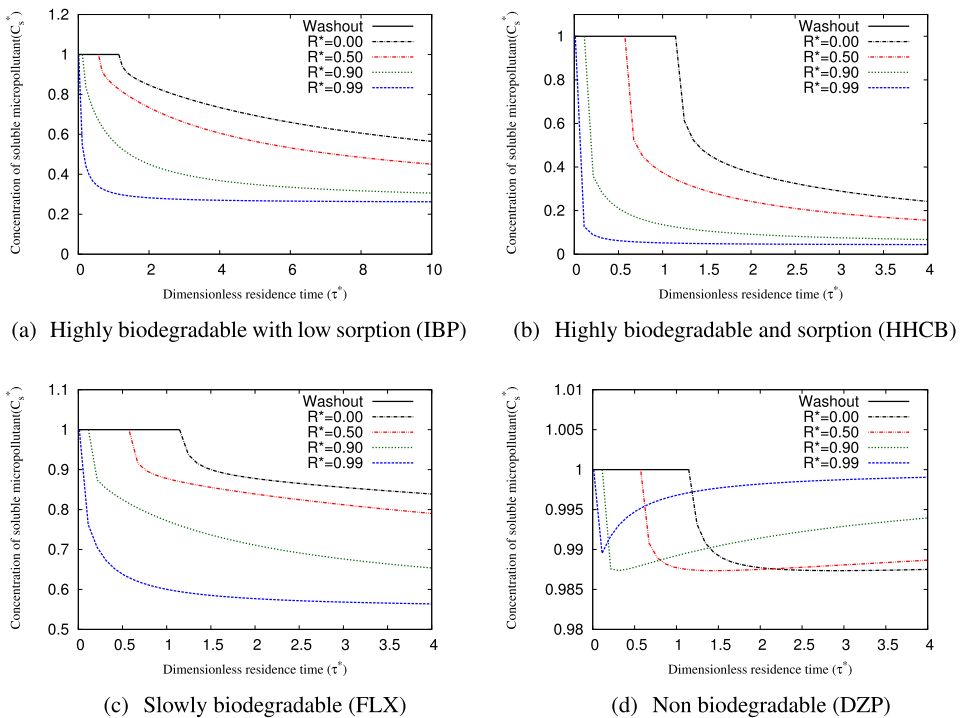
(d) Non biodegradable (DZP)

FIGURE 4. Steady-state diagrams for the dimensionless soluble micropollutant concentration as a function of the effective recycle ratio (colour available online). In each diagram the curve with the highest value of the dimensionless residence time at the transcritical bifurcation corresponds to the case $R^* = 0.0$ and the curve with the lowest value of the dimensionless residence time at the transcritical bifurcation corresponds to the case $R^* = 0.99$. The washout line corresponds to process failure as there is no active biomass in the bioreactor ($X^* = 0$). Parameter values stated in Tables 3 and 4.

the micropollutant is biodegradable, recycle decreases the soluble concentration of micropollutants at intermediate values of the residence time. However, equation (4.11) shows that recycle does not change the limiting value for the soluble concentration of micropollutants.

Figure 4 shows the soluble micropollutant concentrations for four values of the effective recycle ratio ($R^* = 0, 0.5, 0.9, 0.99$). Figure 4(a)–(c) show that concentration of biodegradable micropollutants reduces as the effective recycle ratio is increased. Thus, recycle has a positive effect in reducing the soluble micropollutant concentration. (At sufficiently high values of the residence time the concentration may increase; see discussion of equation (4.14).)

Figure 4(d) illustrates the case when the micropollutant is not biodegradable. In this case, we obtain a surprising result, namely, that the minimum value of the soluble micropollutant concentration is obtained when there is no recycle. This is confirmed by the values shown in Table 6. However, in practice, this effect is likely to be

TABLE 5. The maximum value for the dimensionless particulate micropollutant concentration (C_p^*) and the limiting value for the dimensionless soluble micropollutant concentration (C_s^*).

Compound	τ_{max}^*	$C_{p,max}^*$	$C_s^* (\tau^* \to \infty)$
Highly biodegradable with low sorption			
Ibuprofen (IBP)	2.0391702	0.0047462771	0.25718594
Naproxen (NPX)	2.2118545	0.0042216033	0.36721044
Erythromycin (ERY)	2.2404870	0.0053477151	0.37903397
Roxithromycin (ROX)	2.0918480	0.0076770846	0.28923227
Highly biodegradable with high sorption			
Galaxolide (HHCB)	1.5040588	0.10878801	0.041358696
Tonalide (AHTN)	1.6213181	0.11922515	0.072036863
Slowly biodegradable			
Fluoxetine (FLX)	2.4515015	0.0795152878	0.54970941
Sulfamethoxazole (SMX)	2.5597808	0.0046597008	0.64175347
Trimethoprim (TMP)	2.6462659	0.0074043554	0.72028754
Nonbiodegradable			
Carbamazepine (CBZ)	2.9075954	0.0017853091	1
Diazepam (DZP)	2.9200865	0.0126477035	1

TABLE 6. The dependence of the minimum value of the dimensionless soluble micropollutant concentration (C_s^*) upon the effective recycle parameter for DZP.

R^*	τ_{min}^*	$C_{s,min}^*$
0	2.9201	0.9873522979
0.5	1.4600	0.9873522977
0.9	0.2920	0.9873523123
0.99	0.0292	0.9873539515

insignificant due to the negligible removal of nonbiodegradable micropollutant. Only when the reactor is operated at residence times lower than that at washout ($\tau^* < \tau_{cr}^*(R^* = 0)$) does recycle have a positive effect in reducing the soluble micropollutant concentration.

Figure 5 shows how the recycle affects the particulate micropollutant concentration for the same values of the effective recycle ratio ($R^* = 0, 0.5, 0.9, 0.99$). In all cases, the particulate micropollutant concentration increases as the recycle increases. This is expected, as increasing the effective recycle parameter decreases the amount of particulate matter that is discharged in the waste stream and thereby increasing the amount in the reactor.

(a) Highly biodegradable with low sorption (IBP)

(b) Highly biodegradable and sorption (HHCB)

(c) Slowly biodegradable (FLX)
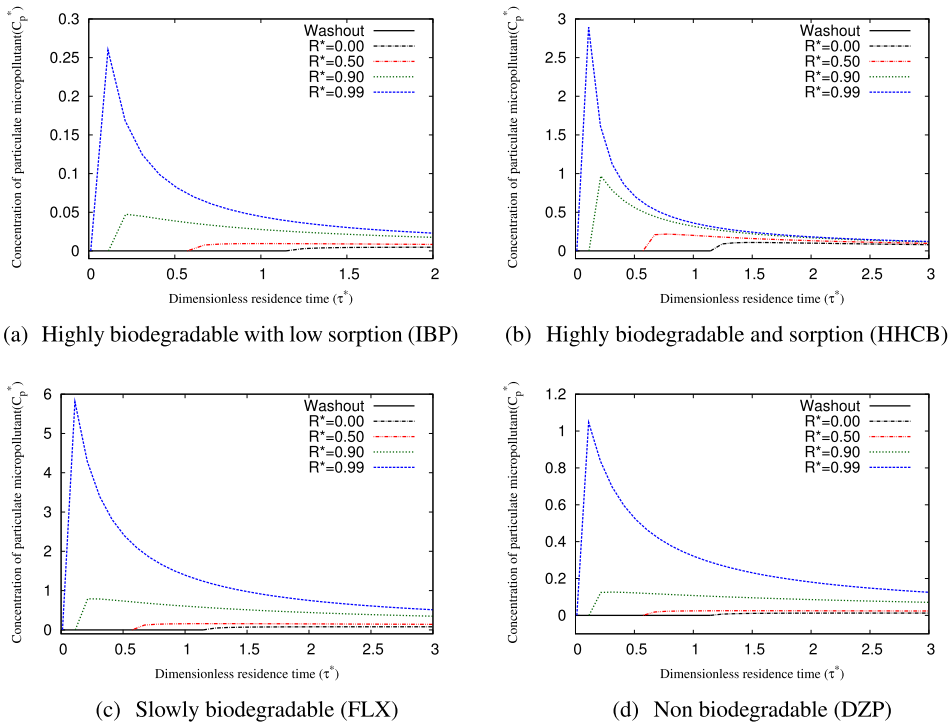
(d) Non biodegradable (DZP)

FIGURE 5. Steady-state diagrams for the dimensionless particulate micropollutant concentration as a function of the effective recycle ratio (colour available online). In each diagram the curve with the highest value of the dimensionless residence time at the transcritical bifurcation corresponds to the case $R^* = 0.0$ and the curve with the lowest value of the dimensionless residence time at the transcritical bifurcation corresponds to the case $R^* = 0.99$. The washout line corresponds to process failure as there is no active biomass in the bioreactor ($X^* = 0$). Parameter values stated in Tables 3 and 4.

Our asymptotic result revealed that the concentration of nonbiodegradable micropollutants is minimized at a finite value of the residence time. This is shown in Figure 2(d). Figure 6 shows a curve in the K_d–k_{sor} parameter space along which the minimum soluble micropollutant concentration is equal to 0.1, representing 90% removal of the micropollutant. In the region above the curve, the minimum soluble micropollutant concentration is less than 0.1. Thus, 90% removal of the micropollutant is only possible for parameter values above the curve. In the region below the curve, the minimum soluble micropollutant concentration is greater than 0.1. Note that this figure is plotted using the dimensional values, K_d and k_{sor}, rather than dimensionless values, K_d^* and k_{sor}^*, to facilitate comparison with the typical values for nonbiodegradable micropollutants shown in Table 4. From this comparison we conclude that 90% removal of nonbiodegradable micropollutants is impossible. Finally, we note that recycle has a negligible effect on the demarcation line as indicated in Table 6.
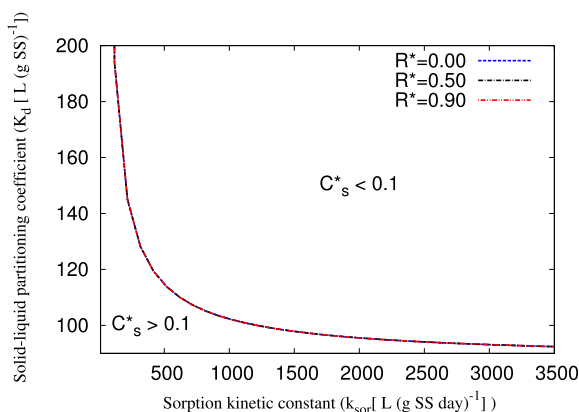
FIGURE 6. Diagram showing that the effective recycle ratio (R^*) has a negligible effect upon the locus $C^*_{s,\min} = 0.1$ in the K_d [L (g SS)$^{-1}$]–k_{sor} [L (g SS day)$^{-1}$] plane for nonbiodegradable micropollutants. For any point on the locus, there is a value of the residence time at which the minimum soluble micropollutant concentration is 0.1. Parameter values stated in Tables 3 and 4.

Figure 7 shows curves in the K_d–k_{sor} parameter space for nonbiodegradable micropollutants along which the soluble micropollutant concentration is equal to 0.5, representing 50% removal of the micropollutant, for different values of the effective recycle ratio. In the region above the curve the soluble micropollutant concentration is less than 0.5. Thus, 50% removal of the micropollutant is only possible for parameter values above the curve. In the region below the curve, the soluble micropollutant concentration is greater than 0.5. Note that recycle now has a significant effect on the location of the boundary.

4.7. Which removal mechanism is the most effective?
At steady state, the rate at which soluble micropollutants enters the reactor (D_1) is given by

$$D_1 = \frac{1}{\tau^*} + \frac{k^*_{sor}}{K^*_d} C^*_p.$$

This expression contains two terms. The first term on the right-hand side of the equation is the rate at which soluble micropollutants enter the reactor in the feed. The second term on the right-hand side is the rate at which micropollutants are generated inside the reactor due to desorption from particulates. There are three processes which lead to a decrease in the concentration of soluble micropollutants.

Rate at which soluble micropollutants leave the reactor in the effluent stream

$$D_2 = \frac{C^*_s}{\tau^*}.$$

Rate at which soluble micropollutants are adsorbed onto particulates
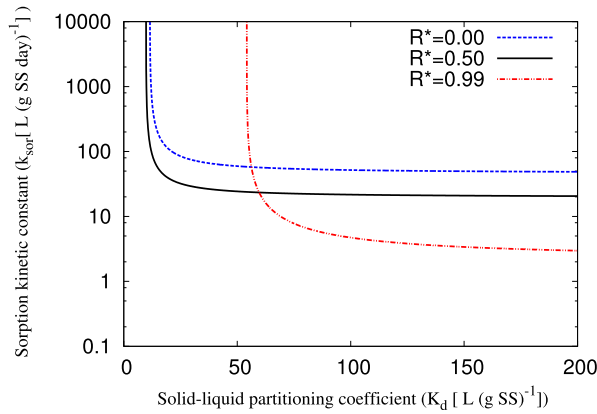
$$D_3 = k^*_{sor} C^*_s X^*.$$

FIGURE 7. Diagram showing how the locus $C_s^* = 0.5$ in the K_d [L (g SS)$^{-1}$]–k_{sor} [L (g SS day)$^{-1}$] plane for nonbiodegradable micropollutant depends upon the value of the effective recycle ratio (R^*) (colour available online). For any point on the locus, there is a value of the residence time at which the minimum soluble micropollutant concentration is 0.5. Parameter values stated in Tables 3 and 4.

Rate at which soluble micropollutants are biodegraded

$$D_4 = k_{\text{biol}}^* X^* C_s^*.$$

At steady state, we have $D_1 = D_2 + D_3 + D_4$. We define the percentage removed in the effluent stream (C), the percentage removed by adsorption (B) and the percentage removed by biodegradation (A) as

$$A = 100\frac{D_4}{D_1}, \quad B = 100\frac{D_3}{D_1}, \quad C = 100\frac{D_2}{D_1}.$$

Figure 8 shows how the percentage removal for each mechanism changes as the dimensionless residence time is changed. Whilst the removal percentages due to biodegradation (A) and due to adsorption (B) are both increasing functions of the residence time, the removal percentage in the effluent stream (C) decreases.

In the vicinity of the washout point, the most important removal mechanism is removal in the effluent stream (mechanism C). At slightly higher values of the residence time the most important removal mechanism is adsorption (mechanism B). This is noteworthy, as in Table 4 IBP is classified as being highly biodegradable with low sorption. In fact, for the parameter values used in this figure biodegradation (mechanism A) is insignificant, never being more than 5.1%. Even at the residence time $\tau^* = 10$, we have $A \approx 5.1\%$. In fact, the percentage removed through adsorption is always higher than that removed by biodegradation.

There is a simple explanation for this finding. The ratio of the percentage removal rate for biodegradation to the percentage removal rate for adsorption is

$$\frac{D_4}{D_3} = \frac{k_{\text{biol}}^*}{k_{\text{sor}}^*}.$$

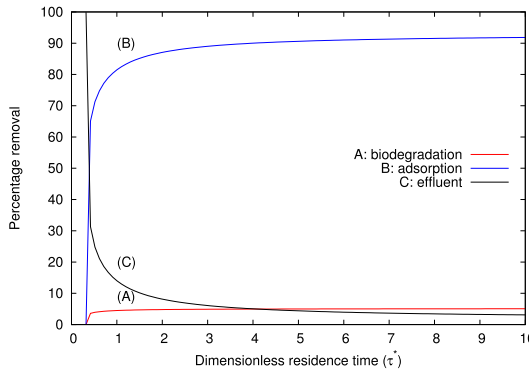Thus, biodegradation is only more effective than adsorption if $k_{\text{biol}}^* > k_{\text{sor}}^*$.

FIGURE 8. The percentage removal of soluble IBP due to: biodegradation ($A = 100(D_4/D_1)$), adsorption ($B = 100(D_3/D_1)$) and removal in the effluent stream ($C = 100(D_2/D_1)$). (Colour available online). The values of the recycle parameter and wastage fraction are $R = 0.4$ and $w = 0.1$, respectively. Parameter values stated in Tables 3 and 4.

At large residence times, the percentage removal by each mechanism is approximately

$$A \approx 100\xi[S_{s,\text{in}}^* - b_H^*(S_{s,\text{in}}^* + 1)]k_{\text{biol}}^* + O\left(\frac{1}{\tau^*}\right),$$

$$B \approx 100\xi[S_{s,\text{in}}^* - b_H^*(S_{s,\text{in}}^* + 1)]k_{\text{sor}}^* + O\left(\frac{1}{\tau^*}\right),$$

$$C \approx 100\xi b_H^*(1 - b_H^*) + O\left(\frac{1}{\tau^*}\right),$$

where

$$\xi = \frac{1}{[S_{s,\text{in}}^* - b_H^*(S_{s,\text{in}}^* + 1)][k_{\text{biol}}^* + k_{\text{sor}}^*] + b_H^*(1 - b_H^*)}.$$

5. Conclusion

We have formulated a mathematical model for the activated sludge process which included the main mechanisms for the removal of micropollutants: biological removal due to biodegradation and/or cometabolism, volatilization and sorption. We considered a simplified model for biotransformation with no cometabolism and representing the rate of biodegradation as a linear function of the concentration of micropollutants.

Experimental evidence indicates that in many circumstances volatilization plays only a minor role in removing micropollutants. Consequently, we removed the volatilization term prior to our analysis. Analytical formulae for the steady-state

TABLE 7. The dimensionless values of the micropollutant biotransformation parameters.

Compound	k^*_{biol}	K^*_d	k^*_{sor}	$\dfrac{K^*_d}{k^*_{\text{biol}}}$, equation (4.14)
Highly biodegradable with low sorption				
Ibuprofen (IBP)	0.010631	0.000681	0.192960	0.0640966
Naproxen (NPX)	0.006343	0.000567	0.260295	0.0893662
Erythromycin (ERY)	0.006030	0.000718	0.072360	0.1190000
Roxithromycin (ROX)	0.009045	0.001079	0.475365	0.1193333
Highly biodegradable with high sorption				
Galaxolide (HHCB)	0.085313	0.032616	6.10337	0.382312
Tonalide (AHTN)	0.047414	0.028293	2.29643	0.596722
Slowly biodegradable				
Fluoxetine (FLX)	0.003015	0.010884	4.169745	3.610000
Sulfamethoxazole (SMX)	0.002055	0.000579	0.149745	0.281739
Trimethoprim (TMP)	0.001429	0.000911	0.193965	0.637031
Nonbiodegradable				
Carbamazepine (CBZ)	0	0.000211	0.087435	∞
Diazepam (DZP)	0	0.001514	0.246225	∞

solutions were then found and their stability was determined as a function of the residence time (hydraulic retention time). Asymptotic solutions for large residence times were provided.

Our steady-state results were used to analyse the the removal of soluble micropollutants. The analysis showed that the removal of soluble micropollutants is optimized when they are highly biodegradable with high sorption. We have shown that in the limit of infinitely large residence time, the concentration of biodegradable micropollutants is independent of the parameter values associated with the processes of adsorption and desorption. The limiting concentration can be minimized by either increasing the value of the biological degradation kinetic constant or concentrating the substrate in the feed. Thus, the removal of biodegradable pollutants can be enhanced by concentrating the feed.

Our asymptotic results show that it is possible that the soluble micropollutant concentration approaches its limiting value from below. For such a compound, there is a finite value of the residence time that optimizes its removal. None of the nine biodegradable micropollutants considered in this study behaved in such a manner.

It follows from our asymptotic results that the removal of nonbiodegradable pollutants is optimized at a finite value of the residence times, as in the limit of infinite residence times their values approach that of the influent.

We found that the use of a settling unit enhances the removal of biodegradable micropollutants (see Figure 4(a)–(c)). However, the use of a settling unit only enhanced the removal of nonbiodegradable micropollutants if the residence time is sufficiently low (see Figure 4(d)). However, in the limit of infinite residence time the value of the soluble micropollutant concentration is independent of the operation of a settling unit. For nonbiodegradable micropollutants, we found a surprising result, namely, that the maximum amount of micropollutant removed may be a decreasing function of the effective recycle ratio. The removal of such micropollutants is, therefore, optimized by not using a settling unit.

We have used our steady-state analysis to investigate the relative effectiveness of the mechanisms by which micropollutants are removed from the reactor. We have shown that the condition for biodegradation to be more effective than adsorption is $k_{\text{biol}}^* > k_{\text{sor}}^*$. The values of these parameters for the micropollutants considered in this paper are provided in Table 7. From this, we see that the condition $k_{\text{biol}}^* > k_{\text{sor}}^*$ never holds.

We conclude that even for the micropollutants described as being "highly biodegradable with low sorption", adsorption is a more effective removal mechanism than biodegradation.

Acknowledgements

Appendix A. Symbols used

In the following we denote the units of S and X by $|S|$ and $|X|$, respectively. The scaled variables are listed at the end of the table.

AHTN	Tonalide	
ASM1	Activated sludge model no. 1	
ASP	Activated sludge process	
C	The recycle concentration factor ($C > 1$)	—
$C_{\max}$	The maximum value of the concentration factor	—
	$C_{\max} = (R + 1)/(R + w)$	

C_g	Gas-phase concentration of micropollutant	μg L^{-1}
C_p	The concentration of particulate micropollutants	μg L^{-1}
$C_{p,\text{in}}$	The concentration of particulate micropollutants in the feed	μg L^{-1}
C_s	The concentration of soluble micropollutants	μg L^{-1}
$C_{s,\text{in}}$	The concentration of soluble micropollutants in the feed	μg L^{-1}
CBZ	Carbamazepine	
COD	Chemical oxygen demand	
DCF	Diclofenac	
DZP	Diazepam	
ERY	Erythromycin	
F	Flow rate through the bioreactor	L day^{-1}
FLX	Fluoxetine	
H	Henry coefficient of the micropollutant	$\dfrac{(\mu\text{g L})_{\text{wastewater}}}{(\mu\text{g L})_{\text{air}}}$
HHCB	Galaxolide	
IBP	Ibuprofen	
K_d	Solid–liquid partitioning coefficient	L (g SS)$^{-1}$
K_{La}	Mass transfer coefficient	(day^{-1})
K_S	Monod constant for heterotrophic biomass	g COD L^{-1}
K_{SC}	Micropollutant affinity constant	μg L^{-1}
M_2	Monod kinetics for readily biodegradable soluble substrate	—
NPX	Naproxen	
Q_{air}	Aeration flow rate	L_{air} day^{-1}
PDE	Partial differential equation	
R	Recycle ratio based on volumetric flow rates	—
ROX	Roxithromycin	
S_s	Concentration of soluble substrate	g COD L^{-1}
$S_{s,\text{in}}$	Substrate concentration in the feed	g COD L^{-1}
SMX	Sulfamethoxazole	
T_C	Micropollutant transformation capacity	μg/(g COD)
TMP	Trimethoprim	
TSS	Total suspended solids	g SS L^{-1}
V	Volume of the bioreactor	L
$X_{B,H}$	Concentration of particulate biomass (heterotrophs)	g COD L^{-1}
$X_{B,H,\text{in}}$	Concentration of particulate biomass (heterotrophs) in the feed	g COD L^{-1}
X_{TSS}	Total suspended solids in the reactor	g SS L^{-1}
Y_H	Heterotrophic yield factor	$\dfrac{\text{g COD L}^{-1}}{\text{g COD L}^{-1}}$
b_H	Heterotrophic decay coefficient	day^{-1}

c_2	Conversion factor from COD to TSS	$\dfrac{\text{g SS}}{\text{g COD}}$
	for component $X_{B,H}$	
k_{biol}	Biological degradation kinetic constant	L (g COD day)$^{-1}$
k'_{biol}	Biological degradation kinetic constant under	day^{-1}
	conditions of constant biomass	
k_c	The maximum rate of biodegradation of the	μg (g COD day)$^{-1}$
	micropollutant when there is no growth substrate	
k_{des}	Desorption kinetic constant	day^{-1}
k_{sor}	Sorption kinetic constant	L (g SS day)$^{-1}$
r_{biol}	Biological removal rate	μg L^{-1} day^{-1}
t	Time	day
w	The fraction of the recycle stream that is wasted	—
μ	Specific growth rate model	day^{-1}
μ_{max}	Maximum specific growth rate for biomass	day^{-1}
τ	Residence time	day
	$\tau = V/F$	
C_p^*	Scaled concentration of particulate micropollutants	—
	$C_p^* = C_p/C_{s,\text{in}}$	
$C_{p,\text{in}}^*$	The concentration of particulate micropollutants	—
	in the feed $C_{p,\text{in}}^* = C_{p,\text{in}}/C_{s,\text{in}}$	
C_s^*	Scaled concentration of soluble micropollutants	—
	$C_s^* = C_s/C_{s,\text{in}}$	
K_d^*	The dimensionless solid–liquid partitioning coefficient	—
	$K_d^* = c_2 K_d Y_H K_S$	
Q_{eff}	The dimensionless effective aeration flow rate	—
	$Q_{\text{eff}} = H Q_{\text{air}}/V \mu_{\text{max}}$	
R^*	Effective recycle parameter	—
	$R^* = (C_{\text{max}} - 1)R$	
S^*	Scaled concentration of soluble substrate	—
	$S^* = S_S/K_S$	
$S_{s,\text{in}}^*$	The dimensionless substrate substrate concentration	—
	in the feed $S_{s,\text{in}}^* = S_{s,\text{in}}/K_S$	
X^*	Scaled concentration of particulate biomass	—
	$X^* = X_{B,H}/(K_S Y_H)$	
X_0^*	Scaled concentration of particulate biomass in the feed	—
	$X_0^* = X_{B,H,\text{in}}/(K_S Y_H)$	
b_H^*	The dimensionless heterotrophic decay coefficient	—
	$b_H^* = b_H/\mu_{\text{max}}$	
k_{biol}^*	The dimensionless biotransformation kinetic constant	—
	$k_{\text{biol}}^* = k_{\text{biol}} Y_H K_S/\mu_{\text{max}}$	
k_{sor}^*	The dimensionless sorption kinetic constant	—
	$k_{\text{sor}}^* = c_2 K_{\text{sor}} Y_H K_S/\mu_{\text{max}}$	

t^*　　　　Scaled time　　　　　　　　　　　　　　　　　　　—

　　　　　$t^* = \mu_{\max,H} \cdot t$

τ^*　　　　Dimensionless residence time　　　　　　　　　—

　　　　　$\tau^* = V\mu_{\max}/F$

τ^*_{cr}　　　Value of the scaled residence time at the transcritical　—
　　　　bifurcation

　　　　　$\tau^*_{\mathrm{cr}} = (1 + S^*_{s,\mathrm{in}})(1 - R^*)/[S^*_{s,\mathrm{in}} - (1 + S^*_{s,\mathrm{in}})b^*_{\mathrm{H}}]$

References

[1]　C. Abegglen, A. Joss, C. S. McArdell, G. Fink, M. P. Schlüsener, T. A. Ternes and H. Siegrist, "The fate of selected micropollutants in a single-house MBR", *Water Res.* **43** (2009) 2036–2046; doi:10.1016/j.watres.2009.02.005.

[2]　J. Alex, L. Benedetti, J. Copp, K. V. Gernaey, U. Jeppsson, I. Nopens, M.-N. Pons, L. Rieger, C. Rosen, J. P. Steyer, P. Vanrolleghem and S. Winkler, "Benchmark simulation model no. 1 (BSM1)", CODEN:LUTEDX/(TEIE-7229) 80-2186, Department of Industrial Electrical Engineering and Automation, Lund University, 1998.
http://www.iea.lth.se/publications/Reports/LTH-IEA-7229.pdf.

[3]　R. Bürger, J. Careaga, S. Diehl, C. Mejías, I. Nopens, E. Torfs and P. A. Vanrolleghem, "Simulations of reactive settling of activated sludge with a reduced biokinetic model", *Comput. Chem. Eng.* **92** (2016) 216–229; doi:10.1016/j.compchemeng.2016.04.037.

[4]　G. Byrns, "The fate of xenobiotic organic compounds in wastewater treatment plants", *Water Res.* **35** (2001) 2523–2533; doi:10.1016/S0043-1354(00)00529-7.

[5]　C. Cadet, V. D. S. Martins and D. Dochain, "Dynamic modeling of clarifier–thickeners for the control of wastewater treatment plants: a critical analysis", in: *19th Int. Conf. System Theory, Control and Computing (ICSTCC), 2015* 571–576; doi:10.1109/ICSTCC.2015.7321354.

[6]　C. E. Cowan, R. J. Larson, T. C. J. Feijtel and R. A. Rapaport, "An improved model for predicting the fate of consumer product chemicals in wastewater treatment plants", *Water Res.* **27** (1993) 561–573; doi:10.1016/0043-1354(93)90165-E.

[7]　C. S. Criddle, "The kinetics of cometabolism", *Biotechnol. Bioeng.* **41** (1993) 1048–1056; doi:10.1002/bit.260411107.

[8]　L. Delgadillo-Mirquez, L. Lardon, J.-P. Steyer and D. Patureau, "A new dynamic model for bioavailability and cometabolism of micropollutants during anaerobic digestion", *Water Res.* **45** (2011) 4511–4521; doi:10.1016/j.watres.2011.05.047.

[9]　S. Diehl, J. Zambrano and B. Carlsson, "Steady-state analysis of activated sludge processes with a settler model including sludge compression", *Water Res.* **88** (2016) 104–116; doi:10.1016/j.watres.2015.09.052.

[10]　S. Diehl, J. Zambrano and B. Carlsson, "Steady-state analyses of activated sludge processes with plug-flow reactor", *J. Environ. Chem. Eng.* **5** (2017) 795–809; doi:10.1016/j.jece.2016.06.038.

[11]　G. A. Ekama, G. I. Bernard, F. W. Gunthert, P. Krebs, J. A. McCorquodale, D. S. Parker and E. J. Wahlberg, *Secondary settling tanks: theory, modelling, design and operation* (IWA, London, 1997).

[12]　E. Fernandez-Fontaina, M. Carballa, F. Omil and J. M. Lema, "Modelling cometabolic biotransformation of organic micropollutants in nitrifying reactors", *Water Res.* **65** (2014) 371–383; doi:10.1016/j.watres.2014.07.048.

[13]　E. Fernandez-Fontaina, F. Omil, J. M. Lema and M. Carballa, "Influence of nitrifying conditions on the biodegradation and sorption of emerging micropollutants", *Water Res.* **46** (2012) 5434–5444; doi:10.1016/j.watres.2012.07.037.

[14] E. Fernandez-Fontaina, I. Pinho, M. Carballa, F. Omil and J. M. Lema, "Biodegradation kinetic constants and sorption coefficients of micropollutants in membrane bioreactors", *Biodegradation* **24** (2013) 165–177; doi:10.1007/s10532-012-9568-3.

[15] F. I. Hai, L. D. Nghiem, S. J. Khan, W. E. Price and K. Yamamoto, "Wastewater reuse: removal of emerging trace organic contaminants", in: *Membrane biological reactors: theory, modeling, design, management and applications to wastewater reuse* (eds F. I. Hai, K. Yamamoto and C. Lee), (IWA, London, 2014) 165–205.

[16] M. Henze, C. P. L. Grady Jr, W. Gujer, G. V. R. Marais and T. Matsuo, "A general model for single-sludge wastewater treatment systems", *Water Res.* **21** (1987) 505–515; doi:10.1016/0043-1354(87)90058-3.

[17] B. N. Jacobsen and E. Arvin, "Biodegradation kinetics and fate modelling of pentachlorophenol in bioaugmented activated sludge reactors", *Water Res.* **30** (1996) 1184–1194; doi:10.1016/0043-1354(95)00259-6.

[18] U. Jeppsson and S. Diehl, "An evaluation of a dynamic model of the secondary clarifier", *Water Sci. Technol.* **34**(5–6) (1996) 19–26; wst.iwaponline.com/content/34/5-6/19.

[19] U. Jeppsson and S. Diehl, "On the modelling of the dynamic propagation of biological components in the secondary clarifier", *Water Sci. Technol.* **34**(5–6) (1996) 85–92; doi:10.1016/0273-1223(96)00632-4.

[20] A. Joss, S. Zabczynski, A. Göbel, B. Hoffmann, D. Löffler, C. S. McArdell, T. A. Ternes, A. Thomsen and H. Siegrist, "Biological degradation of pharmaceuticals in municipal wastewater treatment: proposing a classification scheme", *Water Res.* **40** (2006) 1686–1696; doi:10.1016/j.watres.2006.02.014.

[21] A. M. Karpinska and J. Bridgeman, "CFD-aided modelling of activated sludge systems—a critical review", *Water Res.* **88** (2016) 861–879; doi:10.1016/j.watres.2015.11.008.

[22] B. Li and M. K. Stenstrom, "Research advances and challenges in one-dimensional modeling of secondary settling tanks—a critical review", *Water Res.* **65** (2014) 40–63; doi:10.1016/j.watres.2014.07.007.

[23] B. Li and M. K. Stenstrom, "A sensitivity and model reduction analysis of one-dimensional secondary settling tank models under wet-weather flow and sludge bulking conditions", *Chem. Eng. J.* **288** (2016) 813–823; doi:10.1016/j.cej.2015.12.055.

[24] B. Li and M. K. Stenstrom, "Practical identifiability and uncertainty analysis of the one-dimensional hindered-compression continuous settling model", *Water Res.* **90** (2016) 235–246; doi:10.1016/j.watres.2015.12.034.

[25] Y. Luo, W. Guo, H. H. Ngo, L. D. Nghiem, F. I. Hai, J. Zhang, S. Liang and X. C. Wang, "A review on the occurrence of micropollutants in the aquatic environment and their fate and removal during wastewater treatment", *Sci. Total Environ.* **473–474** (2014) 619–641; doi:10.1016/j.scitotenv.2013.12.065.

[26] H. Melcer, J. P. Bell, D. J. Thompson, C. M. Yendt, J. Kemp and P. Steel, "Modeling volatile organic contaminants fate in wastewater treatment plants", *J. Environ. Eng.* **120** (1994) 588–609; doi:10.1061/(ASCE)0733-9372(1994)120:3(588).

[27] M. I. Nelson, J. L. Quigley and X. D. Chen, "A fundamental analysis of continuous flow bioreactor and membrane bioreactor models with non-competitive product inhibition", *Asia-Pac. J. Chem. Eng.* **4** (2009) 107–117; doi:10.1002/apj.234.

[28] D. Orhon, F. G. Babuna and O. Karahan, *Industrial wastewater treatment by activated sludge*, 1st edn (IWA, London, 2009).

[29] W. J. Parker, H. D. Monteith, J. P. Bell, H. Melcer and P. Mac Berthouex, "Comprehensive fate model for metals in municipal wastewater treatment", *J. Environ. Eng.* **120** (1994) 1266–1283; doi:10.1061/(ASCE)0733-9372(1994)120:5(1266).

[30] M. Pomiès, J.-M. Choubert, C. Wisniewski and M. Coquery, "Modelling of micropollutant removal in biological wastewater treatments: a review", *Sci. Total Environ.* **443** (2013) 733–748; doi:10.1016/j.scitotenv.2012.11.037.

[31] E. Ramin, X. Flores-Alsina, G. Sin, K. V. Gernaey, U. Jeppsson, P. S. Mikkelsen and B. G. Plósz, "Influence of selecting secondary settling tank sub-models on the calibration of WWTP models— a global sensitivity analysis using BSM2", *Chem. Eng. J.* **241** (2014) 28–34; doi:10.1016/j.cej.2013.12.015.

[32] H. Siegrist, A. Alder, W. Gujer and W. Giger, "Behavior and modeling of NTA degradation in activated-sludge systems", *Water Sci. Technol.* **21** (1989) 315–324; http://wst.iwaponline.com/content/21/4-5/315.

[33] J. Struijs, J. Stoltenkamp and D. van de Meent, "A spreadsheet-based box model to predict the fate of xenobiotics in a municipal wastewater treatment plant", *Water Res.* **25** (1991) 891–900; doi:10.1016/0043-1354(91)90170-U.

[34] S. Suarez, J. M. Lema and F. Omil, "Removal of pharmaceutical and personal care products (PPCPs) under nitrifying and denitrifying conditions", *Water Res.* **44** (2010) 3214–3224; doi:10.1016/j.watres.2010.02.040.

[35] I. Takács and G. A. Ekama, "Final settling", in: *Biological wastewater treatment* (eds M. Henze, M. C. M. van Loosdrecht, G. A. Ekama and D. Brdjanovic), (International Water Association Publishing, London, 2008) 309–334; Chapter 12.

[36] I. Takács, G. G. Patry and D. Nolasco, "A dynamic model of the clarification–thickening process", *Water Res.* **25**(10) (1991) 1263–1271; doi:10.1016/0043-1354(91)90066-Y.

[37] E. Torfs, T. Maere, R. Bürger, S. Diehl and I. Nopens, "Impact on sludge inventory and control strategies using the benchmark simulation model no. 1 with the Bürger–Diehl settler model", *Water Sci. Technol.* **71**(10) (2015) 1524–1535; doi:10.2166/wst.2015.122.

[38] E. Torfs, M. C. Martí, F. Locatelli, S. Balemans, R. Bürger, S. Diehl, J. Laurent, P. A. Vanrolleghem, P. François and I. Nopens, "Concentration-driven models revisited: towards a unified framework to model settling tanks in water resource recovery facilities", *Water Sci. Technol.* **75**(3) (2017) 539–551; doi:10.2166/wst.2016.485.

[39] T. Urase and T. Kikuta, "Separate estimation of adsorption and degradation of pharmaceutical substances and estrogens in the activated sludge process", *Water Res.* **39** (2005) 1289–1300; doi:10.1016/j.watres.2005.01.015.

[40] J. Wang, C. P. Huang, H. E. Allen, I. Poesponegoro, H. Poesponegoro and L. R. Takiyama, "Effects of dissolved organic matter and pH on heavy metal uptake by sludge particulates exemplified by copper (II) and nickel (II): three-variable model", *Water Environ. Res.* **71**(2) (1999) 139–147; www.jstor.org/stable/25045190.

[41] R. W. Watts, S. A. Svoronos and B. Koopman, "One-dimensional modeling of secondary clarifiers using a concentration and feed velocity-dependent dispersion coefficient", *Water Res.* **30**(9) (1996) 2112–2124; doi:10.1016/0043-1354(96)00024-3.

[42] G. Xu, F. Yin, Y. Xu and H.-Q. Yu, "A force-based mechanistic model for describing activated sludge settling process", *Water Res.* **127** (2017) 118–126; doi:10.1016/j.watres.2017.10.013.

[43] S.-H. Yoon and S. Lee, "Critical operational parameters for zero sludge production in biological wastewater treatment processes combined with sludge disintegration", *Water Res.* **39**(15) (2005) 3738–3754; doi:10.1016/j.watres.2005.06.015.